AD-A104 270 ATOMIC WEAPONS RESEARCH ESTABLISHMENT ALDERMASTON (EN--ETC F/G 8/11
COMPLEXITY OF SHORT PERIOD P SEISMOGRAMS: WHAT DOES SCATTERING --ETC(U)
JUL 81 A DOUGLAS, J A HUDSON, B J BARLEY

UNCLASSIFIED AWRE-O-3/81 DRIC-BR-79646 NL

1 OF 1
AD A
104270

END
DATE
FILMED
10-81
DTIC

BR79646

UK UNLIMITED

AWRE O 3/81

Copies Received 13.
Date. 31-7-81

LEVEL II

AWRE O 3/81

AD A104270

PROCUREMENT EXECUTIVE – MINISTRY OF DEFENCE

AWRE REPORT No. O 3/81

DTIC ELECTE SEP 16 1981 E

Complexity of Short Period P Seismograms:
What Does Scattering Contribute?

A Douglas, AWRE, Aldermaston

J A Hudson, University of Cambridge

B J Barley, AWRE, Aldermaston

DTIC FILE COPY

81 9 10 223

Available from H.M Stationery Office
PRICE £2.00p NET

UK UNLIMITED

A.W.R.E., Aldermaston, Berks.

July 1981

UK UNLIMITED

Procurement Executive - Ministry of Defence

AWRE, Aldermaston

AWRE [redacted]. 03/81

Complexity of Short Period P Seismograms: What Does Scattering Contribute?

A Douglas
J A Hudson*
B J Barley

*Department of Applied Mathematics and Theoretical Physics, University of Cambridge

UK UNLIMITED

ISBN 0 85518144 3

CONTENTS

SUMMARY

It has been suggested that the coda of short period P seismograms including the precursors to PP can be explained as waves scattered in the crust and uppermost mantle. Such scattering regions must be widespread if they are to contribute arrivals to the seismogram over an interval of several minutes. Also, if the amplitudes of the scattered waves are to be large relative to P and PP, as they appear to be on some seismograms, then this suggests that scattering is strong. If this is true, it is then difficult to see how both simple and complex records could be recorded over almost the same ray path, yet observations show that this is possible.

In this report we review the work that has been done on the complexity of the P coda. The most difficult complex seismograms to explain turn out to be those from deep earthquakes with simple source functions and explosions in which the coda is made up of arrivals with high apparent surface speeds. Such seismograms seem to be best explained on the weak signal hypothesis; the seismograms look complex not because the arrivals in the coda are large but because, for the magnitude of the source, the first arrival is small. In order to explain complex explosion seismograms Douglas et al. (1,2) suggest that direct P has been attenuated by passing through a region of low Q which has been missed by the arrivals in the coda. In order to explain complex seismograms from some deep earthquakes, Barley (3) suggests that these are recorded when the direct P path at the source lies close to a node; P is then small for the magnitude of the source and the later (scattered) arrivals appear to be large by comparison.

Simpson and Cleary (4), however, assert that the weak signal hypothesis, at least as applied by Douglas et al. (1,2), has weaknesses and that strong scattering is the explanation of most complex explosion records. The weak signal hypothesis and the strong scattering hypothesis of complexity are therefore compared here and it is shown that, although scattering may well be responsible for the arrivals in the coda, the evidence is that complex records are recorded when the P amplitude is relatively small rather than the coda relatively large, and that for explosion seismograms low Q is the most likely mechanism reducing P.

The data on precursors to PP are also discussed and it is shown that the precursors which are most easily seen in the P core shadow ($\Delta \approx 100$ to 115°) may also be explained by the weak signal hypothesis; the precursors are prominent simply because of the suppression of P (by the presence of the core) and PP (by anelastic attenuation).

Provided that local scattering is small or absent, scattering probably makes a significant contribution to the complexity of P seismograms only when the standard phases (P, PP, etc) have low amplitude relative to that expected from the magnitude of the source.

1. INTRODUCTION

Short period P seismograms often show many more arrivals than the standard phases listed in travel time-tables and several attempts have been made to explain this complexity (see, for example, references (2), (4), (5) and (6)). Much of the early work concentrated on the analysis of the first half minute or so of the P seismogram (see, for example, references (5) and (6)) but in recent years the study of complexity has been extended to include later arrivals and much effort has been devoted to interpreting the so-called precursors to PP as observed at epicentral distances of around 90° to 115° (see, for example, references (7), (8), (9) and (10)).

Certainly the origin of complexity in some earthquake seismograms is prolonged radiation by the source. Studies of large earthquakes, for instance, have shown that faulting at the focus can last for tens of seconds (11). There is also evidence, particularly from studies of the surface waves generated, that underground explosions, though essentially simple sources that radiate most of their energy in a second or less, can trigger strain release in the surrounding rocks (see, for example, reference (12)); presumably this increases the complexity of the P seismogram. However, no clear demonstration of complexity originating in this way has yet been published.

Another cause of complexity is reverberation in the layering near the source and receiver with, particularly for earthquakes, conversion of S to P (5). Douglas et al. (13) have shown by computational studies that reverberations in parallel-layered models might account for some complexity. Reverberation, however, cannot explain all complex seismograms and there seems to be growing agreement that many arrivals in short period P seismograms are the result of scattering. Thus, Key (14) has shown that scattering by heterogeneous near-surface geology and rough topography in the vicinity of the recording station can make significant contributions to the complexity of seismograms. Greenfield (15) has proposed similar scattering in the vicinity of the epicentre as an explanation for the complexity of some explosion seismograms. Douglas et al. (2) suggest that the most important arrivals in the P coda may be those that are generated by "lateral changes in the structure of the crust and upper mantle" and so are scattered arrivals, and Davies and Julian (16) suggest that scattering by structure in subduction zones may produce the observed coda arrivals. Cleary et al. (9) argue that most of the coda can be attributed to scattering by small random inhomogeneities in the crust and uppermost mantle.

Studies of the lithosphere beneath the NORSAR array indicate variations of up to 20% (with a lower limit of 3%) in the wave speeds in the structure down to 120 km (17); such regions are effective scatterers. There is also evidence for scattering by a layer of lateral heterogeneity in the lower mantle (18,19). Estimates of the thickness of this layer vary from 200 km (20) to 600 km (21) and it may be that roughness on the core-mantle boundary also contributes to the scattered signals (22). The evidence for the scattering layer comes not from a study of the P coda but from the precursors to PKIKP. However, we may expect that if P passes close to the core-mantle boundary there will be evidence in the P seismogram of scattering from this layer.

There is thus considerable evidence of scattering regions in the Earth. However, if scattering does contribute significantly to P signal complexity, it seems unlikely that this is the whole story. For to produce scattered arrivals with amplitude comparable to that of the standard phases P and PP would seem to imply strong scattering (as proposed by King, Haddon and Husebye (10)) and if scattered waves contribute to the seismograms over several minutes, these scattering regions must be widespread. However, if there are widespread regions of strong scatterers at shallow depths in the Earth, then this makes it difficult to explain how simple seismograms can be recorded and particularly how both simple and complex seismograms can be recorded over the same source-station paths, but such seismograms are observed. This illustrates the main difficulty in devising a satisfactory explanation of complexity - how to account for the apparently large amplitudes observed in the coda of some P signals without postulating such a marked variation in the elastic properties of the earth that the effect of these variations should be seen on all seismograms recorded over a given path and on all paths so that no simple signals should be seen.

One way of avoiding this difficulty is to assume that most of the coda arrivals are generated by weak scattering and that this type of arrival is almost always present. Consider now an explosion signal; the first arrival will normally have a much larger amplitude than the scattered arrivals and the seismogram will be simple. If, however, some mechanism reduces the first arrival but does not affect the amplitude of the scattered arrivals, then the seismogram will appear complex. Complex earthquake seismograms could be generated in a similar way. We will refer to this way of accounting for the apparently large amplitude of scattered arrivals relative to the standard phases as the weak signal hypothesis. This hypothesis appears to have been first used to explain complexity by Douglas (23) who suggests that complex earthquake signals are those for which the direct P leaves the source close to a node in the radiation pattern and the later arrivals, principally the reverberations in the crust above the source, produce the coda. For simple signals direct P is large because it leaves the source near an antinode in the radiation pattern and the later arrivals are relatively small. (Douglas (23) discusses mainly the interaction of the source radiation pattern and the layering at the source, although he points out that scattering may also contribute to complexity.) Douglas et al. (1,2) have applied the weak signal hypothesis to explosion seismograms and show evidence that complex seismograms are recorded when the direct P wave is attenuated by a low Q zone that is avoided by many of the later arrivals.

Simpson and Cleary (4) argue that the weak signal hypothesis, at least as applied by Douglas et al. (1,2), does not give a satisfactory explanation of complex explosion seismograms and that complexity depends simply on the degree of heterogeneity of the scattering regions in the crust and upper mantle between the source and receiver; the more intense the scattering, the greater the complexity. The purpose of this report is to try and assess the contributions of scattering to P seismograms and particularly to use what information is available to try and decide whether we are dealing with weak or strong scattering. Most of the earlier investigators of the P coda and of precursors to PP have tended to base their estimates of coda amplitudes on a comparison with the amplitude of P and PP. We wish to show that this has probably led to erroneous conclusions about the structure of the Earth. No doubt different scattering mechanisms predominate on different occasions to produce the P coda. We hope to get as much information as we can on these mechanisms by a detailed study of the observations before trying to fit a model.

In order to help separate the effects of scattering from those of simple reverberation in plane parallel-layered models we make comparisons between observed seismograms and model seismograms computed using simple Earth and source models. Further, as scattering and damping are frequency dependent, these effects can only be investigated satisfactorily if information is available on the variation in amplitude with frequency over as wide a band as possible. We thus make use where possible of broad band seismograms which display ground displacement over a wider range of frequencies than the conventional SP seismogram.

We are not concerned here with complexity due to prolonged radiation at the source and so we restrict ourselves to the analysis of data from simple sources. If a short simple P signal is recorded teleseismically at one station, we regard this as evidence that the source itself is simple. If complex signals are recorded elsewhere from the same source, we assume that the complexity is not attributable to the source alone. A complex record on its own without any indication of the duration of the motion at the source cannot be used to make deductions about the origins of complexity.

For convenience we refer to the minute or so of the seismogram after the first arrival as the P coda, to distinguish this part of the seismogram from the precursors to PP. We begin by looking at complexity in the P coda and then go on to consider the origin of the precursors to PP.

2. THE COMPLEXITY OF THE P CODA

One type of scattered wave that has clearly been shown to contribute to the complexity of seismograms is that generated in the vicinity of the recording station by irregularities of the Earth's surface and the heterogeneity of the surface geology. Key (14) has demonstrated that Rayleigh waves which have been converted from the main P signal by rough topography can make significant contributions to the complexity of seismograms as recorded by a single seismograph. These scattered arrivals have apparent surface speeds that are much less than those of the incident P and so, when the outputs of an array are phased and summed to enhance direct P, the low speed scattered waves are suppressed. When the effect of local scattering is reduced in this way many P wave codas still show complexity and these arrivals, as they are not attenuated by array processing, must have apparent wave speeds close to those of P. It is complexity due to arrivals with high apparent wave speeds that have proved most difficult to explain.

Studies of P seismograms on which the effects of local scattering have been suppressed, or are negligible, have demonstrated that explosion signals are usually simple when observed at several stations covering a wide range of azimuth and distance, whereas the earthquake seismograms may range from very simple to very complex; this contrast between explosion signals and earthquake signals has been observed even when the earthquake and explosion epicentres are close together, as can be seen, for example, by comparing the seismograms of the LONGSHOT explosion recorded at four array stations shown in figure 11 of reference (13), with the seismogram from a nearby earthquake recorded at the same stations shown in figure 7 of reference (2). Such observations can be explained in part using simple stratified models of the Earth and pulse-like earthquake and explosion sources. Marked variations in complexity with azimuth (and distance) shown by earthquake seismograms can be simulated in this way (see, for example, reference (24)). In these model studies of the earthquake source the complexity arises mainly from the reverberations in the source layering of the P and S waves radiated upwards from the source; simple seismograms are recorded at those stations for which the direct P amplitude radiated towards the station is much larger than the amplitude radiated along pP or sP paths.

Most of the characteristics of simple explosion signals can also be simulated; examples of this are shown in figure 7. However, all explosion seismograms modelled in this way are simple because the explosion source used generates no S waves and, being very shallow, the P to pP time is short; the main reverberations are generated by shallow boundaries so they follow close on P.

These model studies demonstrate that the main features of some observed P codas can be reproduced using simple parallel-layered models of the Earth, but that not all complex records can be explained in this way. For example, the complex explosion seismograms that are recorded over certain paths are not explained, nor are the complex codas shown by some deep earthquakes; the foci of the deep earthquakes are well away from the main discontinuities in the crust so that the effects of reverberations in the crustal layers should not be seen until many seconds after onset.

Greenfield (15) has suggested that the complexity of explosion signals is due to scattering, principally by rough topography in the vicinity of the source, of short period Rayleigh waves into P waves. The slowly propagating Rayleigh waves thus retain some energy close to the source for several tens of seconds and this energy is gradually converted to P waves and radiated to teleseismic distances. It seems inescapable that this type of scattering will make a significant contribution to the complexity of some seismograms, just as it does in the reciprocal case of scattering in the vicinity of the receiver.

In a study of complex explosion signals Douglas et al. (1,2) conclude that, in general, complexity is best explained on the weak signal hypothesis. It is suggested that P has been reduced by attenuation on passing through a low Q region which is missed by the arrivals in the coda. On this explanation of complexity the magnitude of the explosion source computed from complex records should be less than that computed from a simple record of the same explosion, the first arrivals of the complex records should show a lower proportion of high frequency energy than those of a simple record, and the coda of complex records should contain a higher proportion of high frequency energy than the first arrival. Douglas et al. (1,2) show explosion seismograms that have these properties.

A similar mechanism to that of Douglas et al. (1,2) is proposed by Davies and Julian (16) who suggest that complex seismograms are recorded when P is reduced by defocussing and so the other arrivals that are not similarly reduced may appear to be large relative to P. Davies and Julian (16) have attempted to explain in this way the variation in complexity of the seismograms recorded from the LONGSHOT explosion as discussed later. This mechanism may also explain the variation in the complexity of P signals across the NORSAR array. Frazier (25) shows that for the same explosion some NORSAR sub-arrays record simple seismograms whereas others record very complex seismograms and that for the sub-arrays that record the simple signals the first arrival is almost an order of magnitude larger than at the sub-arrays that record complex signals. However, the codas of the simple and complex seismograms are of about equal amplitude; only the amplitude of the first arrival differs between the two types of seismogram. The variation in complexity at the NORSAR could thus apparently be explained by assuming that the structure in the upper mantle beneath the NORSAR produces a partial shadow zone at the free surface (Haddon and Husebye (26) have recently determined possible structures that will account for such a shadow zone) and that the coda is generated by scattering into the shadow zone by scatterers both in the crust and upper mantle and at the free surface. So it is the weakness of the first arrival as seen on the complex records rather than the amplitude of the scattered waves that accounts for the complexity. In a later section it is shown that scattering into the shadow cast by the Earth's core may explain the precursors to PP.

Barley (3) uses the weak signal hypothesis to explain the complexity of some deep earthquake seismograms. Deep earthquakes are usually observed to have simple P coda but Barley (3) shows examples of both complex and simple P codas from such earthquakes (depth range 279 to 503 km) as recorded at the Warramunga array (WRA), Australia over virtually constant source-receiver paths. The complex seismograms cannot be due to prolonged radiation by the source as simple seismograms of the same earthquakes are recorded at other stations. Barley (3) presents evidence that the complex records are those for which direct P leaves the source close to a node in the radiation pattern and simple records those for which P leaves close to an antinode. The coda is attributed to scattering, in particular S to P scattering at depths of around 650 km. Because simple and complex signals are recorded over almost the same paths, there is clearly more to explaining the complexity of these deep earthquakes than simply attributing the coda to scattering; the amplitude of P relative to the source magnitude appears to be the main factor controlling complexity.

Although the weak signal hypothesis appears to explain some features of complex seismograms, Simpson and Cleary (4) argue that the hypothesis has weaknesses and that a more consistent interpretation of most complex seismograms is provided by the scattering hypothesis of Cleary, King and Haddon (9) where complexity is attributed to strong scattering at shallow depths. The model proposed by Cleary et al. (9) is shown in figure 1; as well as the P wave that takes the least time path from source to receiver, waves travelling to shorter distances such as D are scattered in the crust and uppermost mantle and some of the scattered waves then follow a least time path to the receiver at R. Reciprocal paths with the source and receiver interchanged are also possible. The amplitude of the scattered waves is assumed to depend mainly on the amplitude of the direct wave arriving at D which, in turn, depends on the decay of P waves with epicentral distance, so the variation in amplitude with time along the P seismogram should follow roughly the form of this amplitude-distance curve. As there is some evidence for a minimum in the amplitude-distance curve at around 10° and a maximum at around 20°, Cleary et al. (9) argue that the P wave seismogram should show a corresponding minimum and maximum at the arrival times of the P waves scattered from these distances. The effect will be blurred somewhat by side-scattering, but it is assumed that the scatterers are large compared with a wavelength and so scattering will be very directional. It must also be assumed that the density of scatterers is fairly uniform over the relevant sections of the crust.

We now look at the objections raised by Simpson and Cleary (4) to the weak signal hypothesis as applied by Douglas et al. (1,2) to explain complex explosion seismograms and try and assess how valid these objections are. We then go on to look at the data presented by Cleary et al. (9) in support of their hypothesis that strong scattering can account for the complexity of the P coda.

2.1 An explosion near Bukhara, USSR

Douglas et al. (1,2) attempt to explain the high frequency arrival following 4 s after P recorded at Gauribidanur (GBA), India ($\Delta = 27.4^{\circ}$) from an explosion near Bukhara, USSR; this high frequency arrival (referred to as P_{H1} by Douglas et al. (1,2)) has amplitude greater than P. The proposed explanation is that P has been attenuated by passing through a region of low Q, whereas P_{H1} has travelled by a path that avoids the low Q and thus has larger amplitude and more high frequency energy than P. Possible paths for P_{H1} suggested by Douglas et al. (1,2) are a PdP path and a diffracted path. Simpson and Cleary (4), however, have pointed out that recent determinations of upper mantle structure make it possible that P_{H1} is generated by a rapid increase in P wave speed at a depth of about 650 km. Because the arrival P_{H1} may have been mis-identified Simpson and Cleary (4) argue that somehow this weakens the arguments of Douglas et al. (1,2). However, the real question is whether P_{H1} is a weak or a strong signal. The seismograms of Johnson (27) and Simpson (see reference (28)) that provide some of the evidence for the rapid increase in wave speed at 650 km show no evidence of an arrival like P_{H1} (both Johnson (27) and Mereu et al. (28) show seismograms recorded at epicentral distances of 27.5° only 0.1° different from the Bukhara-GBA distance) although King and Calcagnile (29) have recently published evidence of such an arrival on paths from USSR to Norway. An explanation of why P_{H1} is seen in some areas but not in others is still required and the effects of variations in the Q structure on P would seem to provide such an explanation. It has been objected that heterogeneity of this sort is too complicated a hypothesis to introduce without other evidence, but Mereu et al. (28) have used just this idea to account for the absence of arrivals of the P_{H1} type in the data of Simpson and it seems difficult to account for the data in any other way.

Further evidence for the low-Q mechanism is provided by the lower frequency of P compared to P_{H1} as seen on the GBA seismograms of the Bukhara explosion. Simpson and Cleary (4) attempt to explain this as an effect of boundary thickness and refer to Nakamura and Howell (30) and Nakamura (31). These papers are concerned with the variation with frequency of the amplitude of a head wave diffracted from a possible transition layer at the base of the crust. The amplitudes decrease sharply as the frequency increases above f_o, where $(f_o H/\Delta\alpha) \simeq 1.7$, H is the thickness of the layer and $\Delta\alpha$ is the change in P wave speed across the layer.

In the proposed structure at 650 km, the "sharp" increase in P wave speed gives a $\Delta\alpha$ of about 1 km/s and an H of about 50 km. Thus, $f_o \simeq 3.4 \times 10^{-2}$ Hz. The actual frequency of the P waves is two orders of magnitude greater than this and so, as would be expected, the head wave will not be observable. It appears that the path followed by P is the optical ray path and no frequency variations will arise unless damping of some sort is present.

2.2 The LONGSHOT explosion

Simpson and Cleary (4) state that one of the features shown by the seismograms from the LONGSHOT explosion recorded in North America is a general decrease in complexity with epicentral distance and that, as the average Q of the upper mantle under North America roughly increases with epicentral distance, the apparent correlation of complexity with Q noted by Douglas et al. (2) is coincidental. This can be checked by looking at the variation in complexity at a fixed distance. Take, for example, the narrow distance range 34 to 37.4^{o} from the LONGSHOT epicentre; this range contains the Canadian stations Prince George, British Columbia (PG-BC), Jasper, Alberta (JP-AT), North Pole, North-West Territories (NP-NT) and Yellowknife (YKA). The first two stations have magnitude (m_b) 4.75 and 5.38 respectively (the LONGSHOT average is 5.8), lie above a region of low Q, and have seismograms which are very complex (see figure 2 for PG-BC, and Key (14) for JP-AT); the last two have magnitude 6.13 and 6.04 respectively, are relatively simple (see Key (14) for YKA and Simpson and Cleary (4) for NP-NT), and lie, according to the weak signal hypothesis, above a region of high Q. It is clear then, that the correlation of complexity with Q cannot be attributed to a distance-related effect.

On the weak signal hypothesis as applied by Douglas et al. (1,2), the complexity of the LONGSHOT records is explained by the reduction of the amplitude of P by a low Q region below the receiver and the relative enhancement of the coda which travels by a separate path avoiding the low Q region. This leads to low m_b, relatively low frequency in the main P signal, and high complexity associated together at a low Q site. On the other hand, high m_b, high frequency P and low complexity will be associated together at a high Q site. These correlations are shown by Douglas et al. (2). The correlation of low m_b, low frequency and low Q is confirmed by Simpson and Cleary (4).

One difficulty with this proposal pointed out by Simpson and Cleary (4) is that most evidence on Q structure indicates that low Q regions are confined to a low-velocity layer in the uppermost mantle. If this layer is reasonably continuous, all arrivals will be attenuated by virtually the same amounts and there will be no paths with less attenuation than on the direct P path, neither for the coda, nor for any subsequent arrivals. However, there is evidence that this is not so. For, although the amplitudes of P on the very complex seismograms recorded at SI-BC (Smithers, British Columbia: $\Delta = 31.8$) and PG-BC ($\Delta = 34.5$) are much less than expected, given the magnitude of LONGSHOT, PcP does not appear to have been similarly reduced; it is in fact much larger than P at these stations (see figure 2). The amplitudes A^c of PcP at SI-BC and PG-BC are 42.5 and 105 nm respectively (32); on the other hand, at YKA, although P is relatively large, A^c is only 38.7 nm and the average value of A^c in the distance range 30 to 35^o is 45 nm.

It appears, therefore, that, although P has been attenuated by low Q, PcP has not and so the low Q zone must be sharply limited in extent. Alternatively, the low Q may be at greater depths in the mantle (as proposed by Douglas et al. (2)) so that the greater attenuation of P is explained by the fact that the P pulse spends much more time in the low Q region than PcP. If there can be two different paths (P and PcP) from the source to the receiver by which the signal is attenuated differently, then there seems to be no reason why there should not be others which will, on the weak signal hypothesis, account for the complexity. Note also that there is evidence from other regions of low Q at depth in the upper mantle; thus, Sacks and Okada (33) report evidence of Q values of 50 and 70 at depths of 400 km beneath Japan and South America.

The signals in the coda arrive, according to Simpson and Cleary (4), by a scattering process from inhomogeneities at shallow depths in the lithosphere. The evidence from the LONGSHOT seismograms, however, is that any scattering in the lithosphere is weak because, as shown above, although at a given station P is complex, PcP is simple. If, nevertheless, we assume that Simpson and Cleary (4) are correct, then in order to account for the early part of the coda, these scatterers must be close to either the source or the receiver. For instance, if the scattered arrivals are to contribute to the first 30 s of the coda, the scatterers must lie within 5^{o} of the station or source and to arrive within 10 s, scattering must take place within 1^{o} of source or station. If the scattering occurs in the vicinity of the station, then the explanation of the early coda is little different from that of Key (14) mentioned earlier. If it takes place near the source, it is similar to Greenfield's (15) explanation of the codas on seismograms of Novaya Zemlya explosions.

If scattering near the source is the explanation of the complex LONGSHOT seismograms, however, the process would have to be very directional because at source the difference in the take off direction of rays going to stations that record complex records and those that record simple records can be quite small. For example, complex P signals would have to have been radiated to stations in British Columbia (eg, SI-BC and PG-BC) and a simple signal to YKA. The difference in azimuth between the British Columbia stations and YKA is only about 18^{o} and the difference in angle between the rays at the Moho below the source is only about 11^{o}; if the surface layer at the source has a P wave speed of about 4 km/s, the angle between the rays at source is about 5^{o}. Similarly, consider the two stations Fort Nelson, British Columbia (FL-BC) and Red Lake, Ontario (RK-ON) which lie on the same azimuth from the source but at distances of 33 and 51.5^{o} respectively. The LONGSHOT seismogram recorded at FL-BC is complex (14) whereas the RK-ON seismogram is simple. At the Moho beneath the source, however, the angular difference between the rays that travel to the two stations is about 6^{o} whereas at the surface the difference is less than 3^{o} (again assuming a P wave speed in the surface layers of 4 km/s).

The scattering of a plane wave (that is, scattering at points far from the source) is fairly directional at high frequencies, but the scattering of a spherical wave (that is, scattering near the source) is not, the incident signal being made up of a superposition of plane waves with different directions of incidence. For instance, high frequency scattering of a spherical wave by a sphere of radius a with its centre a distance d from the source gives, according to the Born approximation, a smoothly varying radiation pattern with a main lobe having semi-angle approximately $\tan^{-1} a/d$. In the case of the inhomogeneities in the lithosphere, a/d appears to have the value of about $\frac{1}{2}$ (17) which makes the lobe semi-angle about 27°, much greater than that required to explain the data.

So far it has been assumed that if the weak signal hypothesis is the explanation of the complexity of the LONGSHOT seismograms, then it is low Q that reduces direct P. Another possible mechanism for reducing P is the presence of a structure that defocusses P and produces a partial shadow zone. Davies and Julian (16) have proposed such a mechanism to explain the variation in the complexity of the LONGSHOT seismograms, the structure causing the defocussing being assumed to be the dipping lithospheric plate, but the fit between the predicted shadow zone and observed regions of low P amplitude is poor. Sleep (34), in a study of five island arcs, concludes that short period amplitude reductions attributable to such shadow zones are not marked (less than a factor of 2). Perhaps then some other structure is responsible for reducing P at the station recording the complex seismogram. However, the assumption that it is low Q rather than defocussing that reduces P seems to be preferable because the relatively low frequency of P as seen at stations that record complex seismograms is then accounted for.

Without array recordings, it is difficult to proceed much further, except to note that the complexity of the LONGSHOT seismograms recorded at single stations in western North America may be due to strong scattering from the mountain ranges of the region, as suggested by Key (14), partly because the scattered waves in this case are Rayleigh waves, slow moving (high energy density) and carrying maximum displacements at the surface.

Apart from the possibility of strong near station scattering from rough topography, it appears that the complexity of the P seismograms from LONGSHOT are most easily accounted for on the weak signal hypothesis.

2.3 Broad band seismograms

Douglas et al. (2) studied several other explosions but these data are not discussed in detail by Simpson and Cleary (14) because they claim that the data "are too few and too disparate for quantitative results to be obtained". However, these data contain a complex explosion signal recorded at an array (that is, a Novaya Zemlya explosion recorded at YKA) on which the effects of local scattering can be attenuated by array processing, thus showing that the complexity is not locally generated. There are few data as useful as this for the purposes of this investigation and so we consider them further here.

First of all, however, we take up the question of how to obtain the maximum information on the variation of amplitudes of a seismogram with frequency. Both scattering and damping are frequency-dependent processes and such information is vital if we are to reach reliable conclusions.

Figure 3 shows the seismograms from an explosion at Novaya Zemlya, USSR (23 August 1975) recorded at YKA ($\Delta = 44.0^{\circ}$) and Eskdalemuir, Scotland (EKA; $\Delta = 28.9^{\circ}$). The relative magnifications of the two types of system used for these recordings are shown as a function of frequency in figure 4. One system (referred to here as the broad band system: BB) has a flat response for displacement from about 0.1 to 10 Hz and is modelled on the response of the Kirnos SKD system (36). The other is a short period (SP) system that is essentially a high pass filter for ground displacement and cuts off sharply below 1 Hz. As we shall show, comparison of the BB and SP versions of the same signal is very revealing.

The BB seismogram for EKA (figure 3(d)) and the SP seismograms for both EKA and YKA (figures 3(a) and 3(f) respectively) were recorded in the form shown in figure 3 and have simply been replayed from tape. No equivalent BB recording is available for YKA so it was necessary to devise a method of constructing the BB seismogram from the SP record. The method used is as follows: at each frequency ω the spectrum of the SP seismogram was multiplied by $a_1(\omega)/a_2(\omega)$, where $a_1(\omega)$ and $a_2(\omega)$ are the responses of the BB and SP systems respectively, and the modified spectrum transformed back to the time domain (this method of obtaining the BB seismogram is based on a suggestion of F A Key (37)). Ideally, this process should produce the required BB seismogram but the process becomes unstable at long periods and additional filtering has to be applied to cut out long period drift. The YKA BB seismogram shown in figure 3(g) has been produced in this way and filtered with a high pass filter that cuts off sharply at frequencies below 0.1 Hz. Also shown in figure 3 is the EKA BB seismogram derived from the SP (figure 3(b)) in the same way as the YKA BB seismogram. The SP to BB conversion and the directly recorded BB (figures 3(b) and 3(d)) are clearly similar, except for the large amplitude low frequency noise shown on the conversion. Figure 3(c) shows the result of applying a Wiener filter to suppress the low frequency noise on the EKA SP to BB conversion. A similar filter has been applied to the directly recorded EKA BB seismogram to reduce the microseisms and this filtered record is shown in figure 3(e). Despite the amount of filtering that has been applied to the original EKA SP seismogram to obtain the estimate of the EKA BB seismogram (figure 3(c)), the conversion shows a striking similarity to the directly recorded broad band signal (figure 3(e)). This gives us confidence that reliable BB seismograms can be obtained from SP seismograms at least for explosions. The same type of Wiener filtering has been applied also to the YKA BB derived from the SP seismogram (figure 3(g)); the result of the filtering is shown in figure 3(h). We now regard this as the BB signal at YKA.

2.4 The Novaya Zemlya explosion

We now consider the evidence provided of the origin of complexity by the SP and BB records of the Novaya Zemlya (NZ) explosion of 23 August 1975 (which appear once more, for ease of comparison, in figure 5). It is clear that the YKA SP seismogram (figure 5(b)) is more complex than for EKA. As displayed the magnification at 1 Hz of the YKA SP seismogram (amplitude of first arrival 102 nm) is about seven times that of the EKA seismogram (amplitude of the first arrival 725 nm). Allowing for this the amplitude of the YKA SP P coda is less than a third the amplitude of the EKA coda. The average amplitude-distance curve for P waves is very nearly constant from 28 to 90^{o} so it is unnecessary to normalise the observed amplitudes at YKA and EKA for distance. Thus, the complexity at YKA appears to be due not to a relatively large coda but to a small P onset since the P coda at EKA is in absolute terms larger than that at YKA. The data presented by Douglas et al. (2) from other NZ explosions recorded at YKA show the same features.

Consider now the YKA BB seismogram (figure 5(d)); when allowance is made for any residual effects of low frequency noise, there is evidence that the BB seismogram is simpler than the SP seismogram. This can most easily be seen over the section AB of the seismogram (figure 5(d)) where the coda is about one-sixth of the maximum amplitude of the signal, whereas on the SP record the amplitude of the coda is about one-third the maximum. This indicates that the coda of the YKA SP seismogram contains more high frequency energy than the first arrival. Further comparison of the EKA and YKA BB seismograms (figures 5(c) and 5(d)) shows clearly that the first arrival at EKA (amplitude 1770 nm) has more high frequency energy than the first arrival on the YKA BB seismogram (amplitude 500 nm). In order to demonstrate that the difference in the amplitude and frequency content of the EKA and YKA BB seismograms can be accounted for by differences in anelastic attenuation on the path to the two stations, the EKA BB seismogram (figure 5(c)) has been passed through a filter to simulate the affects of additional attenuation on the path NZ to YKA. The attenuation at frequency ω due to anelastic attenuation is usually assumed to have the form $\exp(-|\omega| t^*/2)$ where $t^* = T/Q_{AV}$, T is the travel time and Q^{-1}_{AV} the average attenuation factor on the path. If t^*_1 is the value of t^* for the NZ to EKA path and t^*_2 is the value for the NZ to YKA path, then by passing the EKA seismogram through a filter with amplitude response $\exp(|\omega|(t^*_2 - t^*_1))/2$ the resulting seismogram should have the same frequency content as the YKA seismogram at least for the first arrival. Figure 5(e) shows the result of applying such a filter to the EKA BB seismogram with $t^*_2 - t^*_1 = 0.6$ s. (In order to ensure that the filter is causal, it is necessary to include a phase shift; this has been done using the method suggested by Carpenter (38), based on the work of Futterman (39)). The effect of applying such a filter to the EKA BB seismogram is to reduce the amplitude of the first arrival by a factor of 2 (which is about the factor required) and to convert the high frequency first arrival seen on the EKA BB seismogram to a low frequency pulse similar to that seen on the YKA BB seismogram.

Note that the amplitude of PcP on the SP seismogram is much smaller relative to P on the simple EKA record (figure 5(a)) than on the complex YKA record (figure 5(b)), thus giving additional evidence, as on the complex seismograms from LONGSHOT, for the reduction of P relative to the rest of the seismogram. PcP is also small relative to P on the simple seismograms recorded at Gauribidanur (GBA), India from NZ explosions (see figure 7). The ratio A^P/A^C for YKA, EKA and GBA SP seismograms of NZ explosions is roughly 1, 7 and 7 respectively. The PcP phase at YKA as shown on the SP seismogram (figure 5(b)) is about equal in amplitude to P, whereas on the BB seismogram (figure 5(d)) PcP is about half the size of P; this difference in the relative amplitude of P and PcP on the two different types of seismograms shows that P has less high frequency energy than PcP. Comparing the shape of PcP at YKA as seen on the BB seismogram with the shape of P on the EKA BB seismogram shows that anelastic attenuation has affected both these arrivals about equally.

The observations that:-

(a) Direct P recorded at YKA from NZ explosions has lower amplitude than that recorded at EKA.

(b) The coda at YKA has roughly the same amplitude as at EKA.

(c) The proportion of high frequency energy in the BB P signal for YKA is lower than that in the EKA seismogram and that this difference is consistent with the assumption that anelastic attenuation is greater on the paths to YKA than to EKA.

(d) The proportion of high frequency energy in the coda of the YKA BB seismogram is greater than in the first arrival,

are all strong evidence in support of the suggestion of Douglas et al. (2) that the complex seismograms recorded at YKA from NZ explosions arise because direct P has been attenuated by passing through a region of low Q.

The strong scattering hypothesis as applied to these records appears to have the same disadvantages as when applied to the LONGSHOT data. As near station scattering is eliminated as a possible source of complexity, then the early part of the coda must be attributed to scattering close to the source. Such scattering must again be strongly directional, for complex SP seismograms are observed at YKA, Canada (azimuth 353, distance 44^{o}) and other stations in North America, whereas simple seismograms are observed, for example, at EKA, Scotland (azimuth 263.5, distance 29.0^{o}) and GBA, India (azimuth 154.5, distance 61^{o}). However, these stations are widely spread in azimuth so the radiation pattern of scattering is not so tightly constrained as that required to explain the complexity of the LONGSHOT seismogram as near source scattering.

There is a further notable feature of the EKA seismograms shown in figure 5 which is that the BB seismogram shows several arrivals, including PP, which on the SP seismogram are of low amplitude relative to P or are absent; however, the SP seismogram is simpler than the BB. That the SP seismogram is so simple is perhaps surprising because the EKA-NZ distance is 28.9^{o} and so, as with the Bukhara explosion, arrivals due to triplications in the travel time curve are to be expected. King and Calcagnile (29), for example, show SP seismograms recorded at NORSAR from explosions in the USSR (at distances of about 29^{o}) which contain strong arrivals (with amplitude greater than P) about 20 s after onset which they interpret as due to triplication of the travel time curve. The relative amplitude of the arrivals on the EKA BB seismogram compared to the SP shows that the later arrivals contain a much lower proportion of high frequency energy than the first arrival. This conclusion also follows from inspection of the BB seismogram alone where the later arrivals are clearly of lower frequency than P. These differences in the amount of high frequency energy in the later arrivals compared to P suggest that P has followed a path on which the anelastic attenuation is much less than that on not only the paths followed by the scattered waves but also on those followed by the succeeding standard phases. The simplicity of the SP seismogram can thus be confirmed as being due to the effects of Q structure in the crust and upper mantle between EKA and NZ. Mereu et al. (28) illustrate how Q structure can strongly affect the relative amplitudes of such arrivals.

Note that when the EKA BB seismogram is passed through the filter that simulates the effects of anelastic attenuation to produce figure 5(e), the filtered seismogram is more complex than the input to the filter (figure 5(c)). This is because the effect of the filter is to reduce preferentially the high frequency first arrival and leave the later low frequency arrivals almost untouched. This illustrates how a complex record can be produced by reducing or weakening the first arrival. This is the basis of the weak signal hypothesis of complexity.

2.5 Strong scattering and the P coda

Cleary et al. (9) present data from 4 earthquakes and 2 explosions to support their hypothesis that the source of the P coda is strong scattering. One of the paths studied is from Novaya Zemlya to the Warramunga array (WRA: $\Delta = 106^{\circ}$), and another is from the Hindu Kush to Canberra (CAN: $\Delta = 101.8^{\circ}$). For both these paths the influence of the core has to be taken into account and, since in any case these seismograms have more bearing on the precursors to PP than on the coda of P, we shall discuss them in section 3. In this section we are concerned only with the P codas of the other seismograms presented by Cleary et al. (9) which were all recorded at the station CAN and cover the distance range 64.3 to 90.3°; three are from earthquakes and one from an explosion.

It is difficult to assess how well these data support either scattering hypothesis since the possibility of prolonged radiation by the source and scattering in the vicinity of both source and receiver has not been ruled out. No evidence has been presented that any of the earthquakes (all of which have $m_b > 6.0$) have a simple source function. We may suppose as usual that the explosion source is simple, but the question still remains as to the possibility of prolonged near-source scattering along the lines, for instance, of the Greenfield (15) model. The P coda of this seismogram (the CAN record of the CANNIKIN explosion) is more complex than is usual for explosion seismograms, but there is some evidence that the near-source scattering is small because, as Key (14) shows, the signal from the LONGSHOT explosion which was fired at the same test site as CANNIKIN (Amchitka Island in the Aleutians) has a simple P coda as observed at the WRA array. The difference in azimuth from Amchitka Island to

WRA and to CAN is only about 18° and the difference in distance is about 9°, so rays leave the source to these stations along similar paths and it would seem unlikely that any scattering in the source region would not be evident at WRA as well as at CAN. Unfortunately, the array seismograms from the CANNIKIN explosion at WRA are overloaded and we do not have this additional information.

One likely source of complexity in all these four records is scattering from the structure in the neighbourhood of the recording station; CAN is not an array and no example is presented of a simple seismogram to show that the effect of such structure is small. In addition, since the distance between the CANNIKIN firing site and CAN is 90.3°, the ray path for the explosion signal passes close to the core-mantle boundary where there is strong evidence of a scattering layer (see, for example, references (18) and (19)). The contribution to the complexity of the seismogram of scattering within this layer cannot be disregarded.

The main evidence that Cleary et al. (9) find in support of their strong scattering model is that the variation of the P coda amplitudes with time follow roughly the form of the decay of P wave amplitudes with distance. It is inferred that multiple scattering may be neglected and that the process suggested by Greenfield (15), whereby the incident waves are converted by rough topography into surface wave energy and subsequently converted back into body waves, is not effective. In some circumstances, however, this process can be remarkably efficient (35).

The argument for single scattering, even though scattering is not thought to be weak, is that wavelengths are small compared with the size of the inhomogeneities and the scattered waves are highly directional in line with the incident wave; these waves pass through a relatively thin layer at nearly normal incidence and therefore multiple-scattering may be neglected. With wavelengths of about 10 km and observable variations in lithospheric structure of down to 20 km in scale (Aki et al. (17) and confirmed by observation of surface topography) the short wavelength assumption seems rather marginal.

Finally, if the effectiveness of scattering in the upper mantle is strongly regional (as it must be on the strong scattering hypothesis if simple signals are ever to be generated), the variation of the scattered signal with time will reflect the geographical distribution of scatterers more than the amplitude of the incident waves, and any correlation with the amplitude-distance curve will be fortuitous. It may be noted that the weak signal hypothesis does not demand such a restriction on the distribution of scatterers, and since a correlation between the P coda amplitude and the amplitude-distance curve implies a reasonably uniform scattering layer, it is positive evidence for this latter hypothesis.

3. PRECURSORS TO PP

In section 2 it is suggested that, although the P coda is probably largely composed of scattered signals, the main factor controlling complexity is the amplitude of P (and pP and sP) relative to the magnitude of the source. In this section we examine the data on the precursors to PP to see if the apparent prominence of these arrivals can be explained in a similar way.

The precursors to PP have been observed mainly in the distance range 90 to 115°. At these distances some short period P wave seismograms are observed to decay slowly in amplitude until about 80 s before PP, after which time the precursors are seen with amplitudes that are similar to that of P and often larger than PP. Bolt et al. (40) suggest that these arrivals are reflections from the underside of discontinuities in the upper mantle at the mid-point in the path (usually termed PdP) but measurements of the apparent surface speeds (7,9,10) all give values that are either too high or too low for them to be PdP. Further, measurements of the azimuth of arrival show that many of the precursors have azimuths well off great circle paths. These results seem to show conclusively that the arrivals are indeed scattered waves arising from a wide range of sources.

In order to account for the large amplitude of these arrivals relative to P and PP, it seems to have been assumed simply that the scattering is sufficiently intense. The difficulty with assuming that there are widespread regions of intense scattering has been pointed out above. However, the precursors to PP are most clearly seen in the range 95 to 110° which is a shadow zone for P. This suggests that, as with the P coda, the precursors to PP are prominent because direct P is small. We examine this possibility below.

3.1 The model

The model we propose is shown in figure 6; the focus F is assumed to be at a distance greater than about 95° from the receiver R so that the direct P is diffracted along the core-mantle boundary with a resulting reduction in its amplitude. Scattered waves are assumed to be radiated in much the same way as assumed by Cleary et al. (9), although the exact path is not important. All we need to assume is that energy is spreading out from F and that part of this energy is being re-radiated along standard ray paths towards R; these secondary sources will be further and further from F with time. For scatterers close to F the scattered energy is attenuated by diffraction along the core-mantle boundary in a similar way to direct P. However, when the source of the secondary waves reaches some point D, the scattered waves travelling to R miss the core by a sufficient distance to avoid attenuation by diffraction.

In the absence of more detailed information we assume that the loss in amplitude from geometrical spreading and anelastic attenuation along the path FR is about the same as on the path FDR; on the path FR there is further loss of amplitude due to diffraction along the core-mantle boundary and on the path FDR there is loss of amplitude due to the scattering process. Observational evidence on the decay of P waves of frequencies around 1 Hz shows that short period P signals travelling to a distance of greater than about 100° are attenuated by over an order of magnitude compared to P waves travelling to around 90° (see, for example, reference (41)); we assume that this difference in amplitude is due solely to the effects of diffraction along the core-mantle boundary of the P wave travelling to 100° and beyond. Then if equal amplitudes are radiated at source on the paths FR and FD, the scattered waves as seen at R will be of roughly equal amplitude to the direct P if the reduction in amplitude from incident to scattered wave is an order of magnitude. (Here we have discussed the model in terms of great circle paths, but in practice scattering will also take place off such paths. However, the broad conclusion remains.)

During diffraction along the core-mantle boundary the high frequency components of the P signal will be attenuated more rapidly than the low frequency components so P will have less high frequency energy than arrivals that have not travelled along the core-mantle boundary but have had the same anelastic attenuation. Thus, even if scattering is not frequency dependent, the scattered arrivals should have more high frequency energy than direct P. In practice scattering will depend on frequency and the high frequency components will be scattered preferentially. On the final seismogram then the coda should show more high frequency energy than P.

This model for the generation of the precursors is almost identical to that proposed by Cleary et al. (9) and King et al. (10). However, by taking into account the effect of diffraction at the core-mantle boundary, we have no need to involve anything more than weak scattering; these scattered waves are small relative to the primary wave.

So far we have considered scattering only from regions in the crust and upper mantle, yet there is also evidence that there is a scattering region at the base of the mantle (18,19). If this is true, then scattered arrivals are also to be expected following closely on direct P at the distances being considered here ($\Delta = 95$ to 115°) and if the scattered arrivals miss the core, they will be enhanced relative to direct P in much the same way as the waves scattered in the crust and upper mantle.

3.2 The amplitude of PP

If the model outlined above is correct, P is attenuated by diffraction and the arrivals in the coda are relatively low amplitude scattered waves, so that PP might be expected to be large compared to P. Yet the data presented by Cleary et al. (9) shows that the amplitude of PP is less than that of P and is about the same amplitude as the PP precursors. King et al. (10) argue that as the amplitude of PP and the precursors are often roughly equal, this is evidence that the precursors result from strong scattering, but this is not necessarily so as we show in this section.

Consider first P and PP recorded distances of $\Delta < 90^{o}$ so that the P ray path does not interact with the core-mantle boundary and assume that at source P and PP are of equal amplitude, then at frequency ω for sources at shallow depth, P will be attenuated by $\exp(-|\omega|\ t_p^*/2)G(\Delta)$ and PP by $\exp(-|\omega|\ t_{pp}^*/2)\ (G(\Delta/2)/2(\cos\ \Delta/2)^{\frac{1}{2}})\ F(\omega)$. $G(\Delta)$ is the geometrical spreading factor for P to distance Δ. t_p^* is T_P/Q_{AV}^P; T_P is the travel time of P to distance Δ, and $\left(Q_{AV}^P\right)^{-1}$ is the average Q^{-1} for the P ray path. $t_{pp}^* = T_{PP}/Q_{AV}^{PP}$ where T_{PP} is the travel time of PP and $\left(Q_{AV}^{PP}\right)^{-1}$ is the average Q^{-1} for the PP path. $F(\omega)$ is a factor that allows for the effects of reflection at the mid-point of the PP path. If the crust is complicated, then the incident P at the mid-point will be reflected as a series of arrivals with reduced amplitudes. In addition to this, PP will be the Hilbert transform of the incident waves, but for narrow band signals this is unlikely to have much effect on the amplitude.

$F(\omega)$ is difficult to allow for in the frequency domain; the effects are most easily discussed in the time domain. The effect of the reflection at the mid-point of the PP path has therefore been examined by modelling; that is, by an extension of the method of computing theoretical seismograms discussed by Hudson (42,43) and Douglas et al. (13) (see appendix A). These modelling experiments show that for realistic crusts the loss of amplitude at reflection is usually small.

In the range $\Delta = 60$ to 90^{o}, $G(\Delta/2)$ and $G(\Delta)$ are about equal because $G(\Delta)$ as computed from travel time curves (44) is roughly constant in the range 30 to 90^{o} and $(\cos\ \Delta/2^{\frac{1}{2}})$ is about unity so that the geometrical spreading factor for PP is about half that of P. To estimate the differences in the effects of anelastic attenuation for P and PP is difficult. Layers of high anelastic attenuation (low Q) appear to be confined to the upper mantle so as PP spends much more time than P in the upper mantle usually Q_{AV}^{PP} will be less than Q_{AV}^{P}. Also $T_{PP} > T_p$, so, in general, t_p^* will be less than t_{pp}^*.

The observed amplitude-distance curve for P waves in the range 30 to 90^{o} has the same shape as the curve of $G(\Delta)$ computed from travel time tables which implies that t_p^* is roughly constant with distance; so, on average, t_{pp}^*

$= 2t^*_p$. Estimates of t^*_p range from about 0.2 to 1.0 s depending on the path, so t^*_{pp} should be in the range 0.4 to 2.0 s. If $t^*_p = 0.2$ s and t^*_{pp} is 0.4 s, then at 1 Hz PP will be reduced by a factor of 2 relative to P due to anelastic attenuation; for $t^*_p = 1.0$ s and $t^*_{pp} = 2.0$ s the factor is about 20. In practice, the values of t^* for P and PP will not usually be so simply related; there are strong lateral variations in Q in the upper mantle and thus the difference between t^*_p and t^*_{pp} for particular paths will depend very much on the variation of Q with depth in the vicinity of the PP reflection point. However, it does not seem to be unreasonable to expect for some paths a loss of amplitude at 1 Hz due to anelastic attenuation to be an order of magnitude or more for PP than for P, say $t^*_p = 0.2$ s and $t^*_{pp} = 1.0$ s.

If this is true, then on short period seismograms PP could be more than an order of magnitude less than P when observed in the distance range 60 to 90^o, the main factor reducing PP relative to P being anelastic attenuation. On long period seismograms the effects of anelastic attenuation and reflection will be small and so P and PP differences in amplitudes are likely to be less on LP than on SP seismograms and this is supported by observation. For earthquake sources, however, prediction of the relative amplitudes of P and PP is difficult as they will usually have different amplitudes at source.

At distances beyond 95^o direct P is attenuated by diffraction along the core-mantle boundary, whereas PP is not so affected, thus it is not surprising that on an SP seismogram P and PP can be of similar amplitude at these distances. Note that the scattered waves are also assumed to spend more time and travel further in the upper mantle than direct P and so might be expected to be attenuated in the same way as PP. However, as Q varies laterally in the upper mantle and the scattered waves in general have numerous paths to follow, the paths that contribute most to the seismogram will be those on which, other things being equal, attenuation is smallest. For PP, however, the path is fixed so that, if there is low Q on this path, PP will very likely be attenuated much more than its precursors.

3.3 Novaya Zemlya explosions recorded at the Warramunga array

Some of the best examples of precursors to PP are shown by SP seismograms recorded at the Warramunga Array, Australia (WRA) from explosions in Novaya Zemlya, USSR, an epicentral distance of 106^{o} (see, for example, references (7), (9) and (10)). Such a seismogram is shown in figure 7, together with seismograms from an NZ explosion as recorded at Gauribidanur (GBA), India ($\Delta = 60^{o}$). For each station both SP and BB seismograms are shown; the first 150 s of the WRA SP and BB seismograms are shown in figures 7(a) and 7(b) respectively; the continuation of the SP seismogram is shown in figure 7(d) and of the BB seismogram in figure 7(e). The BB seismograms for GBA (figure 7(i)) and both the WRA and GBA SP seismograms (figures 7(a) and 7(g) respectively) were recorded in the form shown and have been simply replayed from tape. No equivalent BB recording is available for WRA so the BB recording shown has been derived from the SP seismogram in the same way as the YKA BB seismograms shown in figure 3(g).

The WRA seismograms are for an explosion on 27 October 1973 whereas the GBA seismograms are for an explosion on 2 November 1974. Ideally the seismograms for the two stations would be for the same explosion but the seismogram for the 1973 explosion is overloaded at GBA and there is no WRA seismogram for the 1974 explosion. However, the seismograms are typical of WRA and GBA seismograms from NZ explosions and there is no reason to suppose that differences in the sources contribute significantly to the observed differences in the complexity of the seismogram. So, in what follows, we assume that the only differences in the seismograms due to differences at source are in absolute amplitude; from comparison with stations that recorded both explosions it seems that the 1973 explosion generated seismic amplitudes about 1.5 times larger than the 1974 explosion. When comparing amplitudes (table 1) the observed GBA amplitudes for the 1974 explosion have been multiplied by 1.5.

The GBA SP seismogram (figure 7(g)) is typical of the simple seismograms usually recorded from explosions; following P, the amplitude falls quickly to about 1/8th of that of P and, apart from PcP, falls steadily from then on so that at the arrival time of PP the amplitude of the seismogram is about

1/20th of P. (Note that this seismogram is from a single (low magnification) seismograph so that some of the coda is probably due to locally generated noise.)

The WRA SP seismogram (figures 7(a) and 7(d)) is much more complex than the GBA SP seismogram (figure 7(g)). The WRA SP seismogram is the sum of the outputs of 10 seismometers of an array; the outputs have been time shifted to bring direct P into phase so the effects of any locally generated noise in the seismogram has thus been reduced. Note that there are arrivals with amplitude up to half the P amplitude or more for about 25 s after onset; the amplitude then decreases slowly until about 2 min after P when the amplitudes increase again giving the so-called precursors to PP. On the seismogram the largest amplitude is PP. (Phasing up the array records to enhance P has partially suppressed PP which has a lower apparent surface speed than P, but tests show that this reduction of PP relative to P is negligible.)

Now consider the broad band seismograms (figures 7(b), 7(e) and 7(i)). The GBA seismogram (figure 7(i)), like the SP version, is simple but PP is now seen with amplitude about 1/8th of P. The differences in the relative amplitude of P and PP on the broad band seismogram compared with the amplitude on the SP seismogram are similar to those shown above by the EKA seismograms of NZ explosions (figures 5(a) and 5(c)) and again indicate that PP has relatively less high frequency energy than P.

The WRA broad band seismogram, after allowance has been made for the presence of low frequency noise, is much simpler than the equivalent SP seismogram. The arrivals following P and preceding and following PP are of lower amplitude on the broad band seismogram relative to PP (and P) than on the SP, showing that these arrivals contain a higher proportion of high frequency energy than either PP or P. Note that on the broad band seismogram PP is nearly three times larger than P, whereas on the SP seismogram PP is only about 1.3 times P. This indicates that, even though P has lost high frequency energy by diffraction along the core-mantle boundary, it still retains more high frequency energy than PP.

The data given above show good agreement with our model. The codas of the GBA and WRA SP seismograms have amplitudes that are roughly equal in absolute amplitude (see table 1) so that it seems reasonable to assume that the main reason that the WRA SP seismogram appears complex is that direct P at WRA has been attenuated by diffraction along the core-mantle boundary, whereas the arrivals following P have not been so attenuated. This is further supported by the observation that the amplitude of PP on the BB seismograms is about equal at GBA and WRA (table 1). The fact that PP is smaller relative to P (and the scattered arrivals) on the SP as compared to the BB seismograms is consistent with our assumption that PP has been more strongly attenuated by anelastic absorption than has P (or the scattered arrivals). A difference in absorption of PP and the arrivals in the WRA seismogram that result from scattering in the crust and upper mantle is to be expected because such scattering would take place in a shield region, and there is evidence that in such regions any low Q layers are either thin or absent, whereas the reflection point of PP is in the Central China fold belt where the average Q of the upper mantle is probably less than in shield regions. This would explain how, on the WRA SP seismograms, PP and the scattered arrivals could be of similar amplitude even though scattering occurred in the lithosphere.

Note that the P coda has a different frequency content to direct P in accordance with the proposed origin of these waves as scattering near the core-mantle boundary. If the coda was generated by scattering in the crust and upper mantle, then this scattering must occur close to the source otherwise the scattered arrivals would not be seen until several tens of seconds after P because of their extended ray paths. However, if the scattering takes place close to the source, the scattered arrivals should follow P and be strongly attenuated by diffraction. Scattering in the lower mantle thus seems to be the best explanation of the P coda. On this explanation of the arrivals in the P coda, weak scattering at or near the core-mantle boundary is probably sufficient to account for the amplitude of the arrivals. The presence of weak rather than strong scatterers in many regions near the core-mantle boundary is also supported by the observation that PcP is usually a simple pulse; the examples shown above of PcP recorded at SI-BC and particularly PG-BC (figure 2) demonstrate this clearly and Davies and Ziolkowski (45) also present evidence that PcP is usually simple.

In order to demonstrate that the GBA and WRA seismograms shown in figure 7 can be explained on a reasonable model of the Earth, an attempt has been made to compute theoretical seismograms. The methods used for the computation of P at distances of less than 95^{o} (and for PcP) are those of Hudson (42,43) and Douglas et al. (13); these methods have been extended using the theory given in the appendices to allow P seismograms at distances of more than 95^{o} and PP seismograms to be computed. The explosion model used is that of Haskell (46) for a 1000 kton explosion in tuff; the depth of the explosion is assumed to be 0.8 km. The details of the crustal models used are given in table 2. The crustal models were obtained by starting with published models and by trial and error modifying these to bring the computed seismograms into closer agreement with the observed. In computing the GBA seismograms the same crustal model was used as for the WRA seismograms; this was done because the model published by Arora et al. (47) for the GBA crust produced model BB seismograms that were more complex in the first 10 s than observed BB seismograms.

Figure 7(h) shows a theoretical SP seismogram computed for GBA. Each phase P, PcP and PP were generated separately and added, together with the appropriate time delay, to give the required seismogram. The relative amplitudes of P and PP are those computed using $t^*_p = 0.2$ s and $t^*_{pp} = 1.0$ s. The amplitude of PcP (computed with $t^* = 0.2$ s) on the other hand has simply been scaled to have an amplitude roughly in agreement with the observed amplitude relative to P. The theoretical BB seismogram for GBA (figure 7(j)) has been computed in the same way.

The theoretical seismograms for WRA are shown in figures 7(c) and 7(f), in which, to allow more realistic comparisons to be made with the observed seismograms, noise with the same properties as the observed seismograms has been added to the theoretical seismograms. This noise was generated by the method of Pearce and Barley (48) using a section of noise preceding the onset of the P signal. The relative amplitude of P and PP shown on the theoretical BB seismograms at WRA have been adjusted (by increasing the theoretical P amplitude by a factor of about 2) so that these relative amplitudes agree roughly with those observed.

Despite the simplicity of the models used the agreement between computed and observed seismograms for the major phases P, PP and PcP seem to be satisfactory. Note that, because of the differences in the values of t* used for P and PP, PP is larger relative to P on the BB seismogram computed for GBA than on the computed SP seismogram in agreement with observation. It is clear that between the standard phases the computed seismograms are simpler than the observed. This difference is always observed and is a measure, at least for explosion sources, of the possible contribution of scattering to observed seismograms. Some of the differences between the observed and computed models presumably arise because the crustal models used are not the best plane layered approximations to the crust and upper mantle structure at the source or the receiver. Also the observed GBA seismograms are from single seismographs and so contain a component of locally generated noise; the remainder is then presumably scattered arrivals from long range. From the observed GBA seismograms given in figure 7 these scattered arrivals from long range appear to have amplitudes of less than 0.1 of the amplitude of P in the first minute after onset and less than 0.05 of the amplitude of P in the second minute after onset.

3.4 Other data on the precursors to PP

The main evidence presented by Cleary et al. (9) in support of the scattering hypothesis is from NZ explosions as recorded at WRA, and this has been discussed above. None of the other seismograms presented by Cleary et al. (9) show any convincing evidence of precursors to PP; this is particularly true of the examples recorded at distances of 90.3^{o}, or less, which are outside the shadow zone of P.

All the clearest examples of precursors to PP appear to have been recorded at distances of 95 to 115^{o} where the presence of the core has to be taken into account; King et al. (10), using three earthquakes as recorded at the NORSAR array (distance range 100 to 105^{o}), have made the most detailed study of them. They show that the arrival times, apparent speeds and azimuths of the precursors are consistent with scattering at distances of 20 to 30^{o} from either source or receiver. The most important scattering region appears to be in the vicinity of the Urals. However, as shown in figure 7, the short period P seismograms from NZ explosions recorded at GBA show no evidence of any precursors, yet this ray path passes under the Urals and remains within 5^{o} of the Urals along its length up to 20^{o} from the source. This suggests that any scattering in the vicinity of the Urals is weak.

King et al. (10) have computed the theoretical root mean square amplitude envelope of the PP precursors for epicentral distances of about 105^{o}. The main feature shown by the theoretical envelopes is a sharp increase in the amplitude of the precursors about 80 s before the arrival of PP. The increase in the theoretical envelope corresponds to the arrival of waves scattered at distances of 20^{o} from source or receiver and arises because of the focussing effect on P waves travelling to 20^{o} of the upper mantle structure used. These computations, however, ignore the effects of the core. On the model we propose an increase in the amplitude of the precursors arises because, with increasing time, scattering takes place further and further from the source (and receiver) so that the core becomes a less and less effective barrier on paths followed by the scattered waves.

4. DISCUSSION AND CONCLUSIONS

From the data presented above we suggest that the following general model explains the properties of most complex P seismograms. We assume that any effects of locally generated noise at the station has been allowed for and that the complexity is not due to prolonged radiation at source. We further assume that weak scattering takes place within the Earth. Between any source and receiver there is thus, as well as the paths followed by the standard phases, numerous paths along which scattered energy travels.

Consider first the case where the losses by geometrical effects and anelastic attenuation along the scattered paths is about the same as on the standard paths. Then, for explosions with uniform radiation patterns, direct P (+pP) will dominate the seismogram and any later scattered arrivals will be small. For earthquakes, provided that the amplitude radiated along the direct P path is close to the peak in the radiation pattern, the seismogram will be dominated by P and possibly the reverberations in the layers at source, and again the scattered arrivals will be small in comparison. If, however, the directions P and pP leave the source lie close to nodes in the radiation pattern, and if sP is also small, then the scattered arrivals generated by radiation from the antinodes of the radiation pattern may be much larger than the standard phases. The coda of the resulting complex seismogram will then be composed almost entirely of scattered arrivals. In this way a seismogram which shows scattered arrivals which have large amplitudes relative to the standard phases and one which has relatively small scattered arrivals can be recorded over the same path.

If now we assume that on some paths there are obstacles that reduce P but not all the scattered arrivals, then complex seismograms will be recorded on this path from either explosions or earthquakes; such paths should always show complex SP seismograms. The obstacles to P may be localised regions of low Q, the Earth's core, or dipping plates and other lateral variations in structure that cause the P wave to diverge forming a partial shadow zone.

The general model to explain complex seismograms given above, which is based on the weak signal hypothesis, avoids the need to assume that there are widespread regions of strong scattering but does not rule out the possibility that there are localised regions of strong scattering. In fact the work of Key (14), which shows that topography in the vicinity of the recording station acts as a strong scatterer, implies by reciprocity that strong scattering by topography will also take place in the vicinity of the source, as suggested by Greenfield (15). (From the data presented in this report, however, we have found no convincing evidence that strong scattering in the source region by rough topography makes a significant contribution to complexity.)

If the weak signal hypothesis is correct, then the distribution of scatterers and their properties remain to be determined. (Some of these arrivals may be reflections from dipping boundaries, as suggested by Wright and Muirhead (7), and it thus becomes a matter of definition as to whether these are described as reflected or scattered arrivals.) The most likely scattering regions, apart from rough topography and heterogeneities due to near surface geology, seem to be the crust and uppermost mantle, as Cleary et al. (9) suggest, but Barley (3) has published evidence of scattering at depths of 650 km and Cleary and Haddon (18) and many others have published evidence of scattering near the core mantle boundary. Some support for the existence of a scattering layer near the core mantle boundary has also been presented in this report. It is also possible that observable scattering takes place throughout the whole of the Earth but for most of the deep interior these effects are small. Note that it is not necessarily true that all arrivals in the coda are the result of lateral variations in the Earth; if there are small variations in the rate of increase of wave speed with depth, then arrivals generated by these variations may add to the coda in the same way as crustal reverberations.

One property of complex P codas pointed out by Douglas et al. (1,2) is that complexity is a function of frequency; the higher the frequency band of the recording, the greater, in general, the observed complexity. Further evidence in support of this suggestion is presented above. Douglas et al. (2) argue that this is evidence that the later arrivals in the coda have followed paths of higher Q than the direct arrival, but if the coda consists of scattered arrivals, the scattering process, being more effective at high frequencies, will give rise to a similar effect. In general, the effects of Q and the scattering process on the distribution of energy with frequency in the coda will be difficult to separate. At long periods scattered arrivals should be less prominant than at short periods. Nevertheless, long period (LP) seismograms do show arrivals between P and PP. Bolt et al. (40) show examples of precursors to PP as seen on LP seismograms from the World Wide Standard Station Network (which they interpret as PdP phases) and conclude that this demonstrates that the precursors have significant energy over a wide spectrum. Ward (49) from a study of the arrivals on LP seismograms between P and PP concludes that these are not scattered arrivals or PdP phases but are reflected and converted phases (S to P and P to S) at discontinuities in the upper mantle close to the source and receiver. Such arrivals may also be present on SP seismograms but are likely to be less significant than on LP seismograms because the upper mantle discontinuities are probably transition zones rather than sharp boundaries and the reflections and conversions at these transition zones at short periods may be of much smaller amplitude than at long periods. (Ward (49), however, shows that arrivals due to S to P conversions at transition zones up to 10 km thick may be significant at 1 Hz and so such arrivals could contribute to the coda of SP seismograms as well.)

Thus, although the arrivals between P and PP would appear to have a wide energy spectrum, in fact they probably consist mainly of scattered waves at short periods and reflected and converted waves at long periods.

REFERENCES

1. A Douglas, P D Marshall and D J Corbishley: "Absorption and the Complexity of P Signals". Nature Phys Sci, 233, 50-51 (1971)

2. A Douglas, P D Marshall, P G Gibbs, J B Young and C Blamey: "P-Signal Complexity Re-Examined". Geophys J R Astr Soc, 33, 195-221 (1973)

3. B J Barley: "The Origin of Complexity in some P Seismograms from Deep Earthquakes". Geophys J R Astr Soc, 49, 773-777 (1977)

4. D W Simpson and J R Cleary: "P-Signal Complexity and Upper Mantle Structure". Geophys J R Astr Soc, 49, 747-756 (1977)

5. H I S Thirlaway: "Earthquake or Explosion?". New Scientist, 18, 311-315 (1963)

6. H I S Thirlaway: "Interpreting Array Records: Explosion and Earthquake P Wave Trains which have Traversed the Deep Mantle". Proc R Soc Lond A, 290, 385-395 (1966)

7. C Wright and K J Muirhead: "Longitudinal Waves from the Novaya Zemlya Nuclear Explosion of 27 October 1966 Recorded at the Warramunga Seismic Array". J Geophys Res, 74, 2034-2048 (1969)

8. C Wright: "Array Studies of Seismic Waves Arriving between P and PP in the Distance Range 90° - 115°". Bull Seis Soc Am, 62, 385-400 (1972)

9. J R Cleary, D W King and R A W Haddon: "P-Wave Scattering in the Earth's Crust and Upper Mantle". Geophys J R Astr Soc, 43, 861-872 (1975)

10. D W King, R A W Haddon and E S Husebye: "Precursors to PP". Physics Earth Planet Int, 10, 103-127 (1975)

11. M Wyss and J N Brune: "The Alaska Earthquake of 28 March 1964: a Complex Multiple Rupture". Bull Seis Soc Am, 57, 1017-1023 (1967)

12. D G Lambert, E A Flinn and C B Archambeau: "A Comparative Study of the Elastic Wave Radiation from Earthquakes and Underground Explosions". Geophys J R Astr Soc, 29, 403-432 (1972)

13. A Douglas, J A Hudson and C Blamey: "A Quantitative Evaluation of Seismic Signals at Teleseismic Distances. III: Computed P and Rayleigh Wave Seismograms". Geophys J R Astr Soc, 28, 385-410 (1972)

14. F A Key: "Some Observations and Analyses of Signal Generated Noise". Geophys J R Astr Soc, 15, 377-392 (1968)

15. R J Greenfield: "Short-Period P-Wave Generation by Rayleigh-Wave Scattering at Novaya Zemlya". J Geophys Res, 76, 7988-8002 (1971)

16. D Davies and B R Julian: "A Study of Short Period P-Wave Signals from LONGSHOT". Geophys J R Astr Soc, 29, 185-202 (1972)

17. K Aki, A Christoffersson and E S Husebye: "Determination of the Three-Dimensional Seismic Structure of the Lithosphere". J Geophys Res, 82, 277-296 (1977)

18. J R Cleary and R A W Haddon: "Seismic Wave Scattering near the Core-Mantle Boundary: a New Interpretation of Precursors to PKIKP". Nature, 240, 549-551 (1972)

19. D W King, R A W Haddon and J R Cleary: "Evidence for Seismic Wave Scattering in the D" Layer". Earth Planet Sci Lett, 20, 353-356 (1973)

20. E S Husebye, D W King and R A W Haddon: "Precursors to PKIKP and Seismic Wave Scattering near the Mantle-Core Boundary". J Geophys Res, 81, 1870-1882 (1976)

21. D J Doornbos: "Characteristics of Lower Mantle Inhomogeneities from Scattered Waves". Geophys J R Astr Soc, 44, 447-470 (1976)

22. D J Doornbos: "On Seismic-Wave Scattering by a Rough Core-Mantle Boundary". Geophys J R Astr Soc, 53, 643-662 (1978)

23. A Douglas: "P-Signal Complexity and Source Radiation Patterns". In Vesiac Report 7885-1-X, University of Michigan (1967)

24. E A Cullen and A Douglas: "P-Wave Seismograms from Three Seismic Sources in SW USSR". Geophys J R Astr Soc, 41, 11-28 (1975)

25. C W Frasier: "Short-Period Amplitude and Waveform Studies at NORSAR". In Seismic Discrimination Semi-Annual Technical Summary, Lincoln Laboratory, MIT (31 December 1972)

26. R A W Haddon and E S Husebye: "Joint Interpretation of P-Wave Time and Amplitude Anomalies in Terms of Lithospheric Heterogeneities". Geophys J R Astr Soc, 55, 19-43 (1978)

27. L R Johnson: "Array Measurements of P Velocities in the Upper Mantle". J Geophys Res, 72, 6309-6325 (1967)

28. R F Mereu, D W Simpson and D W King: "Q and its Effect on the Observation of Upper Mantle Travel-Time Branches". Earth Planet Sci Lett, 21, 439-447 (1974)

29. D W King and G Calcagnile: "P-Wave Velocities in the Upper Mantle beneath Fennoscandia and Western Russia". Geophys J RAstr Soc, 46, 407-432 (1976)

30. Y Nakamura and B F Howell: "Maine Seismic Experiment: Frequency Spectra of Refraction Arrivals and the Nature of the Mohorovicic Discontinuity". Bull Seism Soc Am, 54, 9-18 (1964)

31. Y Nakamura: "Model Experiments on Refraction Arrivals from a Linear Transition Layer". Bull Seism Soc Am, 54, 1-8 (1964)

32. D G Lambert, D H von Seggern, S S Alexander and G A Galat: "The LONGSHOT Experiment. Volumes I and II". Seismic Data Laboratory, Alexandria, Virginia, USA (1969)

33. I S Sacks and H Okada: "A Comparison of the Anelasticity Structure beneath Western South America and Japan". Physics Earth Planet Int, 9, 211-219 (1975)

34. N H Sleep: "Teleseismic P-Wave Transmission through Slabs". Bull Seis Soc Am, 63, 1349-1373 (1973)

35. J A Hudson, R F Humphreys, I M Mason and V K Kembhavi: "The Scattering of Longitudinal Elastic Waves at a Rough Free Surface". J Phys D: Appl Phys, 6, 2174-2186 (1973)

36. P D Marshall, R F Burch and A Douglas: "How and Why to Record Broad Band Seismic Signals". Nature, 239, 154-155 (1972)

37. F A Key: Private Communication

38. E W Carpenter: "Absorption of Elastic Waves - an Operator for a Constant Q Mechanism". AWRE Report O43/66 (1966)

39. W I Futterman: "Dispersive Body Waves". J Geophys Res, 67, 5279-5291 (1962)

40. B A Bolt, M O'Neill and A Qamar: "Seismic Waves near 110°: Is Structure in Core or Upper Mantle Responsible?". Geophys J R Astr Soc, 16, 475-487 (1968)

41. D C Booth, P D Marshall and J B Young: "Long and Short Period P Wave Amplitudes from Earthquakes in the Range 0° - 114°". Geophys J R Astr Soc, 39, 523-537 (1974)

42. J A Hudson: "A Quantitative Evaluation of Seismic Signals at Teleseismic Distances. I: Radiation from Point Sources". Geophys J R Astr Soc, 18, 233-249 (1969)

43. J A Hudson: "A Quantitative Evaluation of Seismic Signals at Teleseismic Distances. II: Body Waves and Surface Waves from an Extended Source". Geophys J R Astr Soc, 18, 353-370 (1969)

44. E W Carpenter: "A Quantitative Evaluation of Teleseismic Explosion Records". Proc R Soc Lond A, 290, 396-407 (1966)

45. D Davies and A Ziolkowski: "Observations of Short-Period Seismic Energy from Earthquakes and Inferences about the Seismic Source". Geophys J R Astr Soc, 31, 131-139 (1972)

46. N A Haskell: "Analytic Approximation for the Elastic Radiation from a Contained Underground Explosion". J Geophys Res, 72, 2583-2587 (1967)

47. S K Arora: "Crustal Structure near Gauribidanur Array". In the Proceedings of a Symposium on the Use of Gauribidanur Data for Seismological Research. Published by Bhabha Atomic Research Centre, Bombay, pp4-36 (1969)

48. R G Pearce and B J Barley: "The Effects of Noise on Seismograms". Geophys J R Astr Soc, 48, 543-547 (1977)

49. S N Ward: "Long-Period Reflected and Converted Upper-Mantle Phases". Bull Seis Soc Am, 68, 133-153 (1978)

50. R W Hurley: "Anomalous Seismic Signals from Novaya Zemlya". AWRE Report O21/77 (1977)

51. G C Werth and R F Herbst: "Comparison of Amplitudes of Seismic Waves from Nuclear Explosions in Four Mediums". J Geophys Res, 68, 1463-1475 (1963)

52. T V McEvilly: "Central US Crust - Upper Mantle Structure from Love and Rayleigh Wave Phase Velocity Inversion". Bull Seis Soc Am, 54, 1997-2015 (1964)

53. P D Marshall, A Douglas, B J Barley and J A Hudson: "Short Period Teleseismic S Waves". Nature, 253, 181-182 (1975)

APPENDIX A

THE COMPUTATION OF PP SEISMOGRAMS

The Fourier transform of the vertical component P seismogram recorded at distance Δ and azimuth ϕ at the free surface is, from refererence (43), equation 7.10,

$$\bar{U}_Z^P(0) = S_V(\omega) C_Z^P(\omega) M^P(\Delta) F^P(i_P, \phi, \omega) \exp\left[- |\omega| \int \frac{ds}{2Q_\alpha \alpha} - i\omega T_P \right],$$

where $S_V(\omega)$ is the response of the seismograph at frequency ω, $C_Z^P(\omega)$ is the response of the layering at the receiver and depends on the angle of incidence (i_P^R) at the base of the layers as well as ω. The term $M^P(\Delta)$ includes the effects of geometrical spreading $G(\Delta)$ and is defined in full by Douglas et al. (13) $F^P(i_P, \phi, \omega)$ is the P wave amplitude radiated at angle i_P (to the vertical) and azimuth ϕ into the halfspace below the source. Finally, ignoring the exp $(-i\omega T_P)$ term which is simply a time shift due to travel time through the mantle, the only remaining term is $\exp(-|\omega| \int ds/2Q_\alpha \alpha$ which allows for anelastic attenuation and following usual practice can be replaced by $\exp(-|\omega| t_P^*/2)$ where t_P^* is defined in section 3.

The vertical component of the PP seismogram $\bar{U}_Z^{PP}(0)$ recorded at (Δ, ϕ) can be written

$$U_Z^{PP}(0) = \pm i S_V(\omega) C_Z^P(i_{PP}^R, \omega) C^{PP}(i_{PP}^I, \omega) M^{PP}(\Delta) F^P(i_{PP}, \phi, \omega)$$

$$\exp(-|\omega| t_{PP}^*/2) \exp(-i\omega T'_{pp});$$

the expression takes the positive sign when ω is positive and the negative sign when ω is negative. i_{pp} is the take off angle and T'_{pp} the travel time of PP. The term $C^{PP}(i_{pp}^I, \omega)$ allows for the effects of reflection in the crustal layering at the mid-point of the PP path and is given by

$$C^{PP}(i_{PP}^I, \omega) = \left\{ \frac{(J'_{11} + J'_{21})(J'_{32} - J'_{42}) - (J'_{12} + J'_{22})(J'_{31} - J'_{41})}{F'(k, \omega)} \right\}_{k = \omega \sin i_{pp}/\alpha'}.$$

Hudson (43) gives expressions for the quantities J_{ij} and $F(k, \omega)$ in terms of the densities and P and S wave speeds in the crustal layers at the receiver; J'_{ij} and $F'(k, \omega)$ are defined in the same way while the prime indicates that the densities and wave speeds used are now those of the crustal layering at the PP reflection point rather than those of the receiver layers. α'_{PP} is the P wave speed in the half space at the PP reflection point. The term $M(\Delta)$ is given by

$$\overset{PP}{M}(\Delta) = \overset{P}{M}(\Delta)\, G(\Delta/2) \Big/ \left[2G(\Delta)\, \{\cos\,(\Delta/2)\}^{\frac{1}{2}}\right]$$

and $\exp(-\,|\omega|\, t^{*}_{PP}/2)$ is defined in section 3.

APPENDIX B

THE COMPUTATION OF THE SEISMOGRAMS OF DIFFRACTED P

It is assumed that the P ray path just grazes the core at distance $\Delta = 96^\circ$. In order to compute the diffracted P seismogram at distance $\Delta'(\Delta + \Delta_D)$, the P seismogram for distance Δ (= 96°) is first computed by the method described by Douglas et al. (13) using the theory of Hudson (42,43). This P seismogram is then passed through a filter with response at frequency ω of $AC(\omega)$ where

$$A^2 = \left(1 - \frac{r_c \alpha'_c}{\alpha_c} \right) \left(\frac{r_c \sin \Delta}{4\pi A_q^4 \, \alpha_c \, \sin \Delta' \, \left| d^2T/d\Delta^2 \right|} \right)$$

and

$$C^2(\omega) = \exp \left\{ \Delta_D (\omega r_c/2\alpha_c)^{\frac{1}{3}} \, 3^{\frac{1}{2}} q \right\} / (\omega r_c/2\alpha_c)^{\frac{1}{3}}.$$

Note that this filter introduces no phase shift and so is non-causal.

r_c = radius of the core,

α_c = P wave speed at the base of the mantle,

α'_c = $d\alpha/dr$ at the base of the mantle; r is the radial distance from the centre of the Earth (the numerical value of α'_c is taken as $5 \times 10^{-5}\ s^{-1}$),

$d^2T/d\Delta^2$ = second derivative of the P travel time curve at distance $\Delta = 96^\circ$ (the numerical value is taken as 27.25 s/radian/radian),

A_q = 0.70121,

q = -2.33810.

TABLE 1

P and PP Amplitudes and P/PP Amplitude Ratios for Novaya Zemlya Explosions

	P Amplitude, nm	Amplitude of PP or Amplitude of Coda at PP Time, nm	Ratio of Amplitude of P to PP
GBA SP	2030*	100	20
WRA SP	93*	116	0.8
GBA BB	7726*	1288	6.0
WRA BB	617*	1700	0.36

*From reference (50).

WRE amplitudes are for the Novaya Zemlya explosion of 27 October 1973. GBA amplitudes are 1.5 times the amplitudes observed from the Novaya Zemlya explosion of 2 November 1974.

TABLE 2

Crustal Models Used in Computation of Seismograms

	P Wave Speed, km/s	S Wave Speed, km/s	Density, g/cm³	Thickness, km
A. Source Crust				
1st Layer	4.8		2.7	4.2
2nd Layer	6.7		2.8	20.0
Half Layer	8.1		3.3	∞
B. Crust at PP Reflection Point				
1st Layer	3.0	1.66	2.35	5.0
2nd Layer	6.1	3.5	2.7	9.0
3rd Layer	6.4	3.68	2.9	9.0
4th Layer	6.7	3.94	2.9	18.0
Half Space	8.15	4.75	3.3	∞
C. Receiver Crust				
1st Layer	5.6	3.2	2.8	8.6
2nd Layer	5.9	3.4	2.8	12.0
3rd Layer	6.2	3.6	3.2	15.25
Half Space	8.3	4.8	3.4	∞

Note: where the S-wave speed (β) is not given it is assumed that $\beta = \alpha/\sqrt{3}$ where α is the P wave speed.

Crust A is based on Nevada Test Site (Granite Crust) of reference (51).

Crust B on the Standard Continental Crust with Sediment of reference (52).

and Crust C on the crustal model for the Warramunga array site published by Marshall et al. (53).

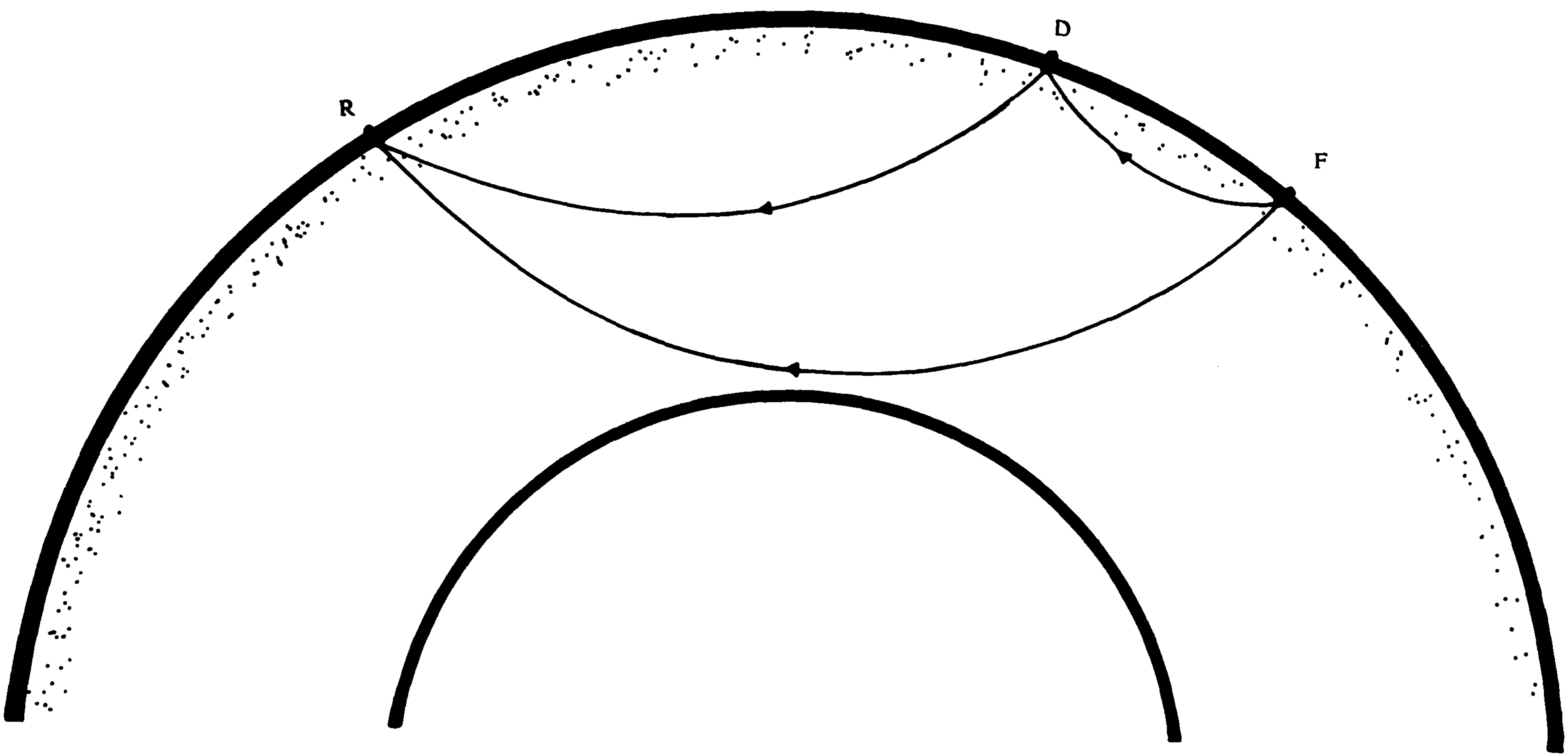

FIGURE 1 Cross-section through the earth showing paths followed by scattered waves according to Cleary et al. (9). F is the source, R the receiver. Some of the energy arriving at D from F is assumed to be radiated towards R.

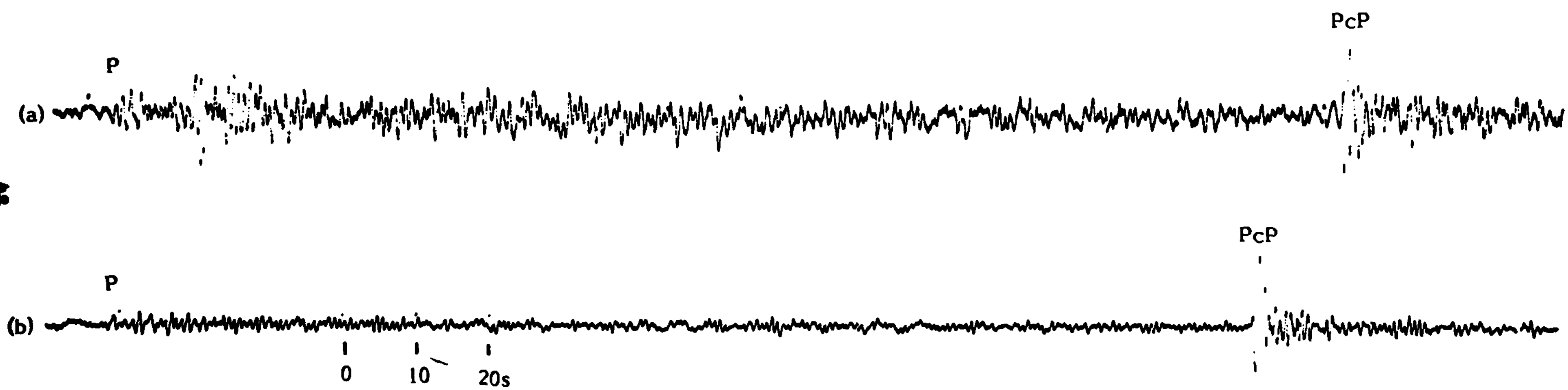

FIGURE 2 Short period P wave seismograms from the LONGSHOT explosion recorded at:-

(a) Smithers, British Columbia (SI-BC).

(b) Prince George, British Columbia (PG-BC).

Note that PcP has a much larger amplitude on both these seismograms than P.

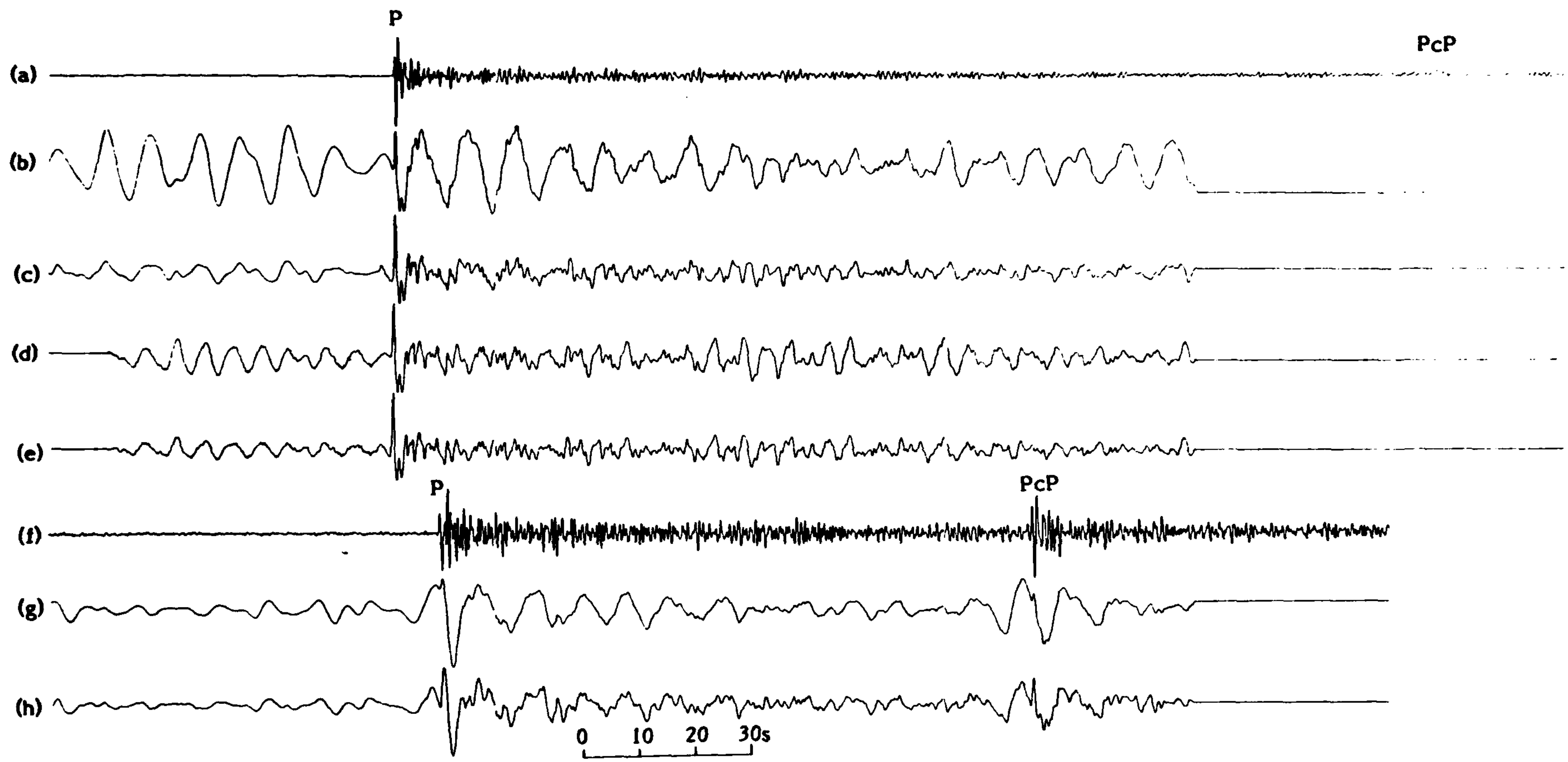

FIGURE 3 P wave seismograms from the Novaya Zemlya explosion of 23 August 1975:-

(a) Short period P seismogram recorded at Eskdalemuir, Scotland.

(b) Broad band P seismogram for Eskdalemuir, Scotland derived from the short period seismogram (a).

(c) Broad band P seismogram (b) after filtering to reduce low frequency noise.

(d) Broad band P seismogram recorded at Eskdalemuir, Scotland.

(e) Broad band P seismogram (d) after filtering to reduce the low frequency noise.

(f) Short period P seismogram recorded at Yellowknife, Canada.

(g) Broad band P seismogram for Yellowknife, Canada derived from the short period seismogram (f).

(h) Broad band P seismogram (g) after filtering to reduce the low frequency noise.

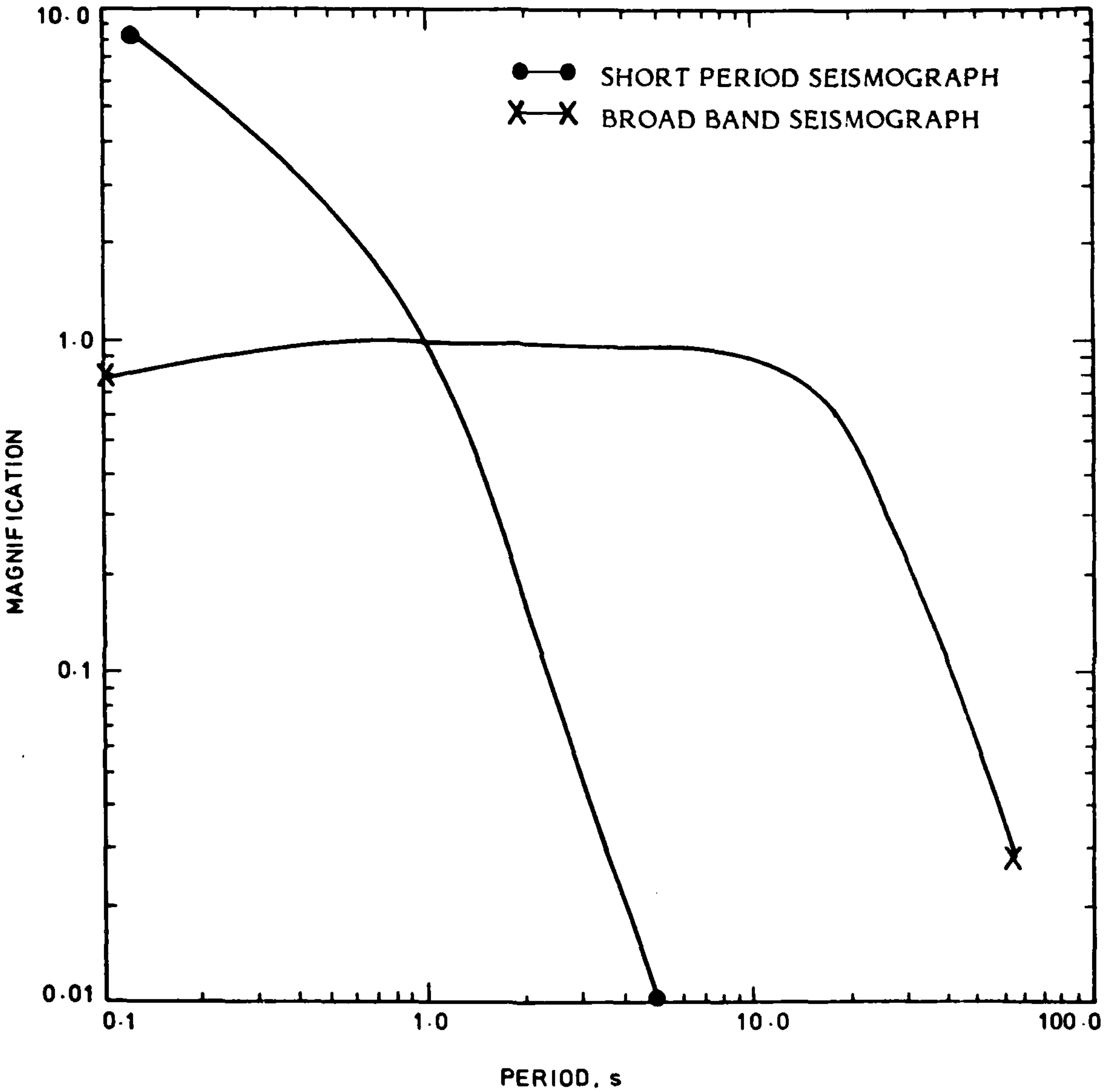

FIGURE 4 Relative magnification of short period (SP) and broad band (BB) seismograph.

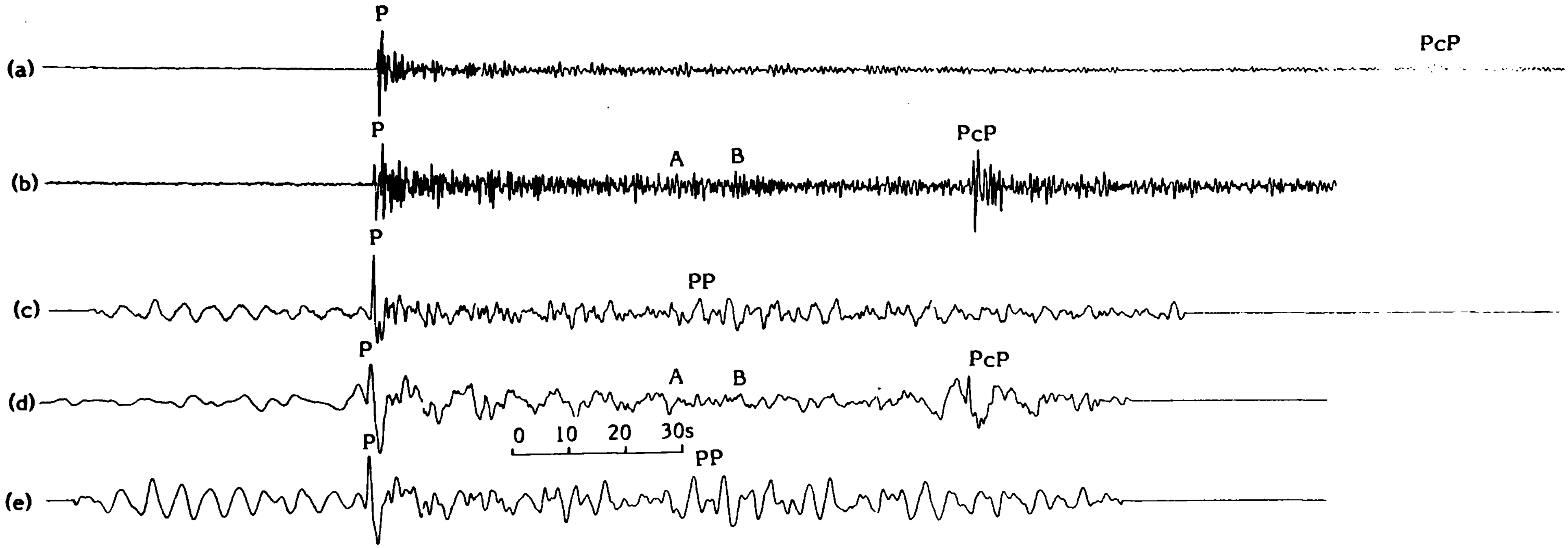

FIGURE 5 P wave seismograms from the Novaya Zemlya explosion of 23 August 1975:-

(a) Short period P seismogram at Eskdalemuir, Scotland.

(b) Short period P seismogram at Yellowknife, Canada.

(c) Broad band P seismogram at Eskdalemuir, Scotland.

(d) Broad band P seismogram at Yellowknife, Canada.

(e) Broad band P seismogram for Eskdalemuir, Scotland (c) after filtering with a filter to simulate anelastic attenuation on the path Novaya Zemlya to Yellowknife, Canada.

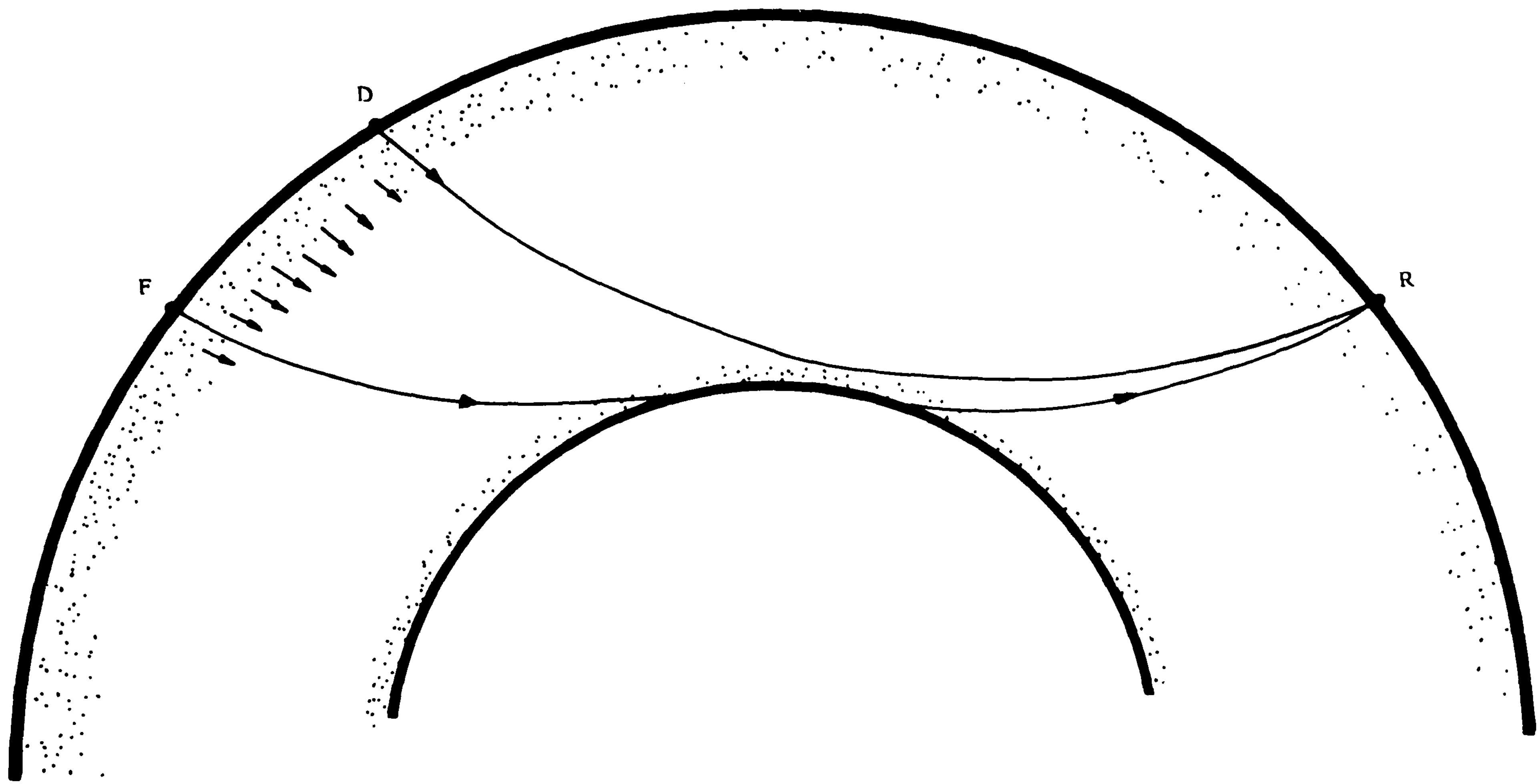

FIGURE 6 Cross-section through the earth showing suggested paths followed by precursors to PP: F is the source, R the receiver. When scattering reaches D ray paths to R no longer intersect the core-mantle boundary.

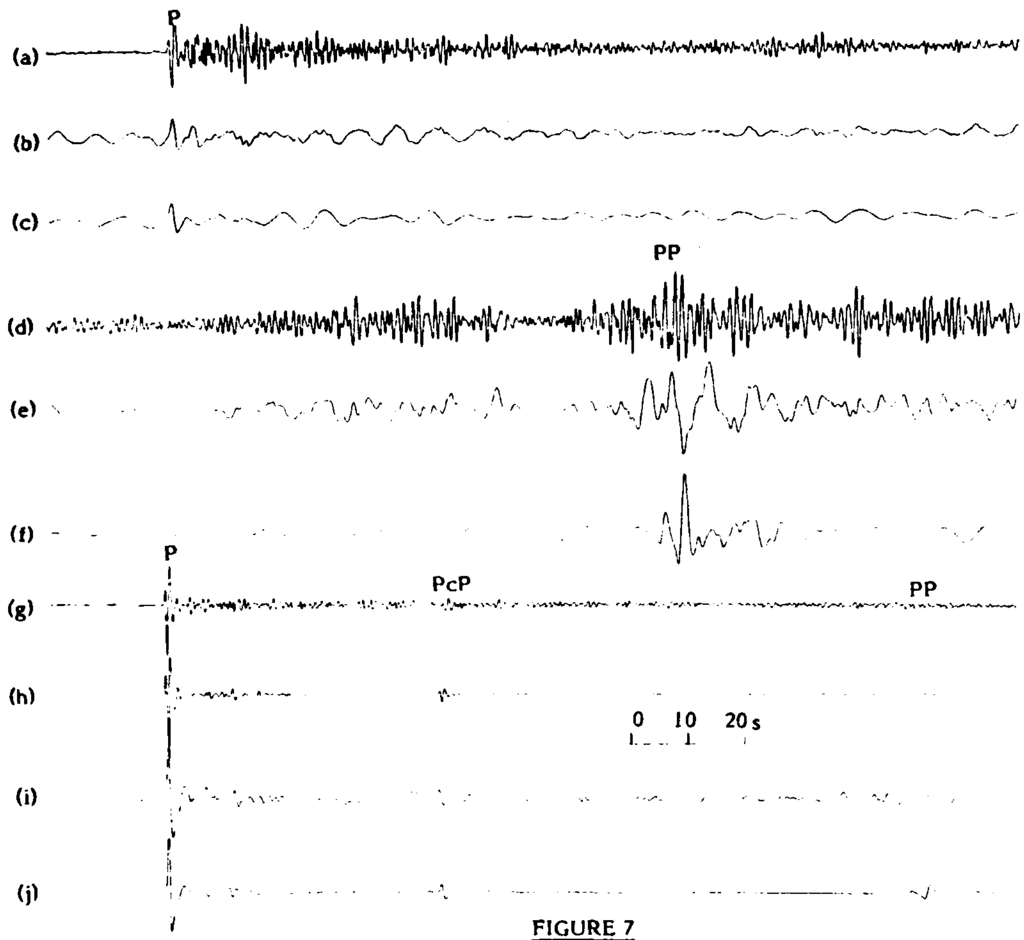

FIGURE 7

(a) Short period P seismogram for Novaya Zemlya explosion of 27 October 1973 recorded at WRA.

(b) Broad band P seismogram for Novaya Zemlya explosion of 27 October 1973 recorded at WRA (derived from SP).

(c) Computed P seismogram (with added noise) to simulate (b).

(d) Short period PP seismogram for Novaya Zemlya explosion of 27 October 1973 recorded at WRA.

(e) Broad band PP seismogram for Novaya Zemlya explosion of 27 October 1973 recorded at WRA (derived from SP).

(f) Computed PP seismogram (with added noise) to simulate (e).

(g) Short period P seismogram for Novaya Zemlya explosion of 2 November 1974 record at GBA.

(h) Computed seismogram to simulate (g).

(i) Broad band P seismogram for Novaya Zemlya explosion of 2 November 1974 recorded at GBA.

(j) Computed seismogram to simulate (i).

DOCUMENT CONTROL SHEET

Overall security classification of sheet ........UNCLASSIFIED..

(As far as possible this sheet should contain only unclassified information. If it is necessary to enter classified information, the box concerned must be marked to indicate the classification eg (R), (C) or (S)).

1. DRIC Reference (if known) -	2. Originator's Reference AWRE Report No. O3/81	3. Agency Reference -	4. Report Security Classification UNLIMITED
5. Originator's Code (if known) -	6. Originator (Corporate Author) Name and Location Atomic Weapons Research Establishment, Aldermaston, Berkshire		
5a. Sponsoring Agency's Code (if known) -	6a. Sponsoring Agency (Contract Authority) Name and Location -		
7. Title Complexity of Short Period P Seismograms. What Does Scattering Contribute?			
7a. Title in Foreign Language (in the case of Translation) -			
7b. Presented at (for Conference Papers). Title, Place and Date of Conference -			
8. Author 1.Surname, Initials Douglas A	9a. Author 2 Hudson J A	9b. Authors 3, 4 .... Barley B J	10. Date pp ref July 1981 54 53
11. Contract Number -	12. Period -	13. Project -	14. Other References -
15. Distribution Statement No restrictions			
16. Descriptors (or Keywords) (TEST) Seismographs Seismic Detection Earthquakes			

Abstract

A review of work done on the complexity of the P coda. The weak signal hypothesis and the strong scattering hypothesis of complexity are compared and data on precursors to PP are discussed.

Some Metric and SI Unit Conversion Factors

(Based on DEF STAN 00-11/2 "Metric Units for Use by the Ministry of Defence", DS Met 5501 "AWRE Metric Guide" and other British Standards)

Quantity	Unit	Symbol	Conversion
Basic Units			
Length	metre	m	1 m = 3.2808 ft 1 ft = 0.3048 m
Mass	kilogram	kg	1 kg = 2.2046 lb 1 lb = 0.45359237 kg 1 ton = 1016.05 kg
Derived Units			
Force	newton	$N = kg\ m/s^2$	1 N = 0.2248 lbf 1 lbf = 4.44822 N
Work, Energy, Quantity of Heat	joule	J = N m	1 J = 0.737562 ft lbf 1 J = 9.47817×10^{-4} Btu 1 J = 2.38846×10^{-4} kcal 1 ft lbf = 1.35582 J 1 Btu = 1055.06 J 1 kcal = 4186.8 J
Power	watt	W = J/s	1 W = 0.238846 cal/s 1 cal/s = 4.1868 W
Electric Charge	coulomb	C = A s	-
Electric Potential	volt	V = W/A = J/C	-
Electrical Capacitance	farad	F = A s/V = C/V	-
Electric Resistance	ohm	Ω = V/A	-
Conductance	siemen	$S = 1\ \Omega^{-1}$	-
Magnetic Flux	weber	Wb = V s	-
Magnetic Flux Density	tesla	$T = Wb/m^2$	-
Inductance	henry	H = V s/A = Wb/A	-
Complex Derived Units			
Angular Velocity	radian per second	rad/s	1 rad/s = 0.159155 rev/s 1 rev/s = 6.28319 rad/s
Acceleration	metre per square second	m/s^2	1 m/s^2 = 3.28084 ft/s^2 1 ft/s^2 = 0.3048 m/s^2
Angular Acceleration	radian per square second	rad/s^2	-
Pressure	newton per square metre	$N/m^2 = Pa$	1 N/m^2 = 145.038×10^{-6} lbf/in^2 1 lbf/in^2 = 6.89476×10^3 N/m^2
	bar	bar = $10^5\ N/m^2$	- 1 in. Hg = 3386.39 N/m^2
Torque	newton metre	N m	1 N m = 0.737562 lbf ft 1 lbf ft = 1.35582 N m
Surface Tension	newton per metre	N/m	1 N/m = 0.0685 lbf/ft 1 lbf/ft = 14.5939 N/m
Dynamic Viscosity	newton second per square metre	$N\ s/m^2$	1 $N\ s/m^2$ = 0.0208854 $lbf\ s/ft^2$ 1 $lbf\ s/ft^2$ = 47.8803 $N\ s/m^2$
Kinematic Viscosity	square metre per second	m^2/s	1 m^2/s = 10.7639 ft^2/s 1 ft^2/s = 0.0929 m^2/s
Thermal Conductivity	watt per metre kelvin	W/m K	-
Odd Units*			
Radioactivity	becquerel	Bq	1 Bq = 2.7027×10^{-11} Ci 1 Ci = 3.700×10^{10} Bq
Absorbed Dose	gray	Gy	1 Gy = 100 rad 1 rad = 0.01 Gy
Dose Equivalent	sievert	Sv	1 Sv = 100 rem 1 rem = 0.01 Sv
Exposure	coulomb per kilogram	C/kg	1 C/kg = 3876 R 1 R = 2.58×10^{-4} C/kg
Rate of Leak (Vacuum Systems)	millibar litre per second	mb l/s	1 mb = 0.750062 torr 1 torr = 1.33322 mb

*These terms are recognised terms within the metric system.

DATE

ILME